NASA/TM–2013-217799

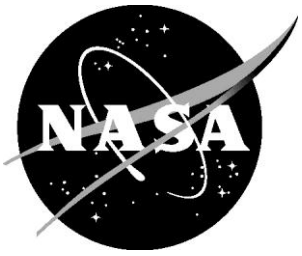

Ultrasonic Nondestructive Evaluation of PRSEUS Pressure Cube Article in Support of Load Test to Failure

Patrick H. Johnston
Langley Research Center, Hampton, Virginia

May 2013

NASA STI Program . . . in Profile

Since its founding, NASA has been dedicated to the advancement of aeronautics and space science. The NASA scientific and technical information (STI) program plays a key part in helping NASA maintain this important role.

The NASA STI program operates under the auspices of the Agency Chief Information Officer. It collects, organizes, provides for archiving, and disseminates NASA's STI. The NASA STI program provides access to the NASA Aeronautics and Space Database and its public interface, the NASA Technical Report Server, thus providing one of the largest collections of aeronautical and space science STI in the world. Results are published in both non-NASA channels and by NASA in the NASA STI Report Series, which includes the following report types:

- TECHNICAL PUBLICATION. Reports of completed research or a major significant phase of research that present the results of NASA Programs and include extensive data or theoretical analysis. Includes compilations of significant scientific and technical data and information deemed to be of continuing reference value. NASA counterpart of peer-reviewed formal professional papers, but having less stringent limitations on manuscript length and extent of graphic presentations.

- TECHNICAL MEMORANDUM. Scientific and technical findings that are preliminary or of specialized interest, e.g., quick release reports, working papers, and bibliographies that contain minimal annotation. Does not contain extensive analysis.

- CONTRACTOR REPORT. Scientific and technical findings by NASA-sponsored contractors and grantees.

- CONFERENCE PUBLICATION. Collected papers from scientific and technical conferences, symposia, seminars, or other meetings sponsored or co-sponsored by NASA.

- SPECIAL PUBLICATION. Scientific, technical, or historical information from NASA programs, projects, and missions, often concerned with subjects having substantial public interest.

- TECHNICAL TRANSLATION. English-language translations of foreign scientific and technical material pertinent to NASA's mission.

Specialized services also include organizing and publishing research results, distributing specialized research announcements and feeds, providing information desk and personal search support, and enabling data exchange services.

For more information about the NASA STI program, see the following:

- Access the NASA STI program home page at *http://www.sti.nasa.gov*

- E-mail your question to help@sti.nasa.gov

- Fax your question to the NASA STI Information Desk at 443-757-5803

- Phone the NASA STI Information Desk at 443-757-5802

- Write to:
  STI Information Desk
  NASA Center for AeroSpace Information
  7115 Standard Drive
  Hanover, MD 21076-1320

NASA/TM–2013-217799

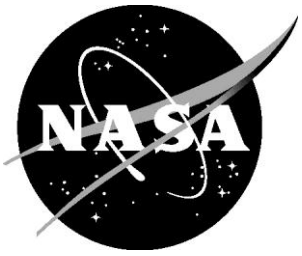

Ultrasonic Nondestructive Evaluation of PRSEUS Pressure Cube Article in Support of Load Test to Failure

Patrick H. Johnston
Langley Research Center, Hampton, Virginia

National Aeronautics and
Space Administration

Langley Research Center
Hampton, Virginia 23681-2199

May 2013

Available from:

NASA Center for AeroSpace Information
7115 Standard Drive
Hanover, MD 21076-1320
443-757-5802

1.0 Introduction

The PRSEUS Pressure Cube Test [1] is a joint development effort between the Boeing Company and NASA Langley Research Center, sponsored in part by the Environmentally Responsible Aviation Project (ERA) and Boeing internal R&D. This Technical Memorandum presents the results of ultrasonic inspections in support of the PRSEUS Pressure Cube Test, and is a companion document with the NASA test report [2] and a report on the acoustic emission measurements made during testing [3]. Portions of the content of these Technical Memoranda were reported at the 2012 Aircraft Airworthiness and Sustainment Conference [4].

2.0 Background

2.1 Pultruded Rod Stitched Efficient Unitized Structure (PRSEUS) Concept

The PRSEUS concept, depicted in Fig. 2.1, has been developed as a low-cost, lightweight composite structure for aircraft [5,6], which offers advantages over traditional metallic structure. The PRSEUS concept is comprised of a stitched carbon fiber-epoxy material system with the potential for reducing the weight and cost of transport aircraft structure by eliminating fasteners. By adding unidirectional carbon rods to the top of stiffeners, the panel becomes more structurally efficient. The combination of stitching with the pultruded rod-reinforced stiffener produces a more damage tolerant material system.

Some key features of the PRSEUS concept are: the improved stiffness provided by the pultruded rod; the crack-arresting nature of the stitches, which enables the use of failsafe design principles; reduced tooling size and weight enabled by the self-supporting nature of the stitched preform; and improved resin infusion through the use of Controlled Atmospheric Pressure Resin Infusion (CAPRI). A photograph of the stiffener side of a flat PRSEUS test panel is shown in Fig. 2.2 [5].

Of note for this paper are the areas where the flanges are folded out from the vertical components (stiffeners, frames, end caps) to mate with the horizontal skin layers. These wedge-shaped volumes were loosely filled with linear bundles of fibers prior to laying down the skin layers, to provide some volume fraction of fibers. These linear areas are referred to as the "noodle" because of the resemblance of the placement of fiber material during manufacture to the laying down of floppy thin cooked noodles.

2.2 Pressure Box Test Article

The key test article for part of the ERA Program is a future full-scale multibay structure, representing the passenger compartment and luggage compartment of a notional aircraft fabricated using PRSEUS panels. The test article for the present study (Fig. 2.3) was a smaller cube-like structure representing all the major features of the multibay structure, including crown, floor, rib panels and bulkhead panels. The main goal of this test was to verify the functionality of the joint design under pressure loading.

The detailed structure of various component parts of the cube is presented in Figures 2.4 through 2.6. Each of the sides was a PRSEUS panel, having seven or eight stringers and two frames. Along the edges, end caps were provided as mating surfaces to fasten and seal to the adjoining face sheets.

2.3 Test Sequence

The test sequence was defined in a test specification document [1]. The test sequence is presented in Table 1.

The Test Specification Document stated that NASA would be responsible for completing the items listed below. In general, NASA would perform test set-up, conduct the test and perform post-test evaluation:

1. Inspect the assembly to ensure the pressure cube was not damaged and that fasteners are still torqued, or to find loose strain gages.
2. Set up testing.
3. Pre & post test photos and video.
4. Prepare the specimen OML surface for VIC-3D (Video Image Correlation in 3 Dimensions) system.
5. Install LVDT's.
6. Conduct the testing per test specification & procedure defined in Section 5. This includes leading the test and recording of all the data.
7. **Perform pre-damage infliction NDI inspection**
8. Impact panel with BVID
9. **Perform post-impact NDI inspection**
10. **Perform post-test evaluation and post-test NDI inspection**

The following sections will describe the highlighted NDI actions.

3.0 Ultrasonic Phased Array Inspection Methods

The flat surface of the PRSEUS panel provided a good interface to use a linear ultrasonic array with a solid plastic wedge, attached to a manually-operated X-Y encoder fitted with suction cups, as shown in Fig. 3.1. An area of approximately 20" X 20" could be inspected in approximately 20 minutes, including the time for positioning the scanner. A 10 MHz linear phased array (64 elements, each 10 mm X 0.5 mm) was used with an aperture of 16 elements. A zero-degree wedge was employed, and the beam was perpendicular to the inspection surface and focused approximately 2 mm below the surface of the composite. Water was sprayed on the panel surface to provide adequate acoustic coupling.

Early success of this method was demonstrated during mechanical testing of flat PRSEUS panels in a load frame [7].

4.0 Ultrasonic NDE Results

4.1 Impact Site

As a part of the damage tolerance testing of the PRSEUS cube, a site was selectively inflicted with barely visible impact damage (BVID). Ultrasonic NDE was performed before and after the BVID to quantify the extent of damage produced by the impact.

Figure 4.1 presents C-scan views of the impact site before and after the impact. An orange oval illustrates the site of impact. The post-impact data show an area of indentation, and a

surrounding brighter area, corresponding to delaminations, which were not observed in the pre-impact data.

A close-up of the impact area is presented in Fig. 4.2. The lateral extent of the delamination is shown to be approximately 1.5 inches by 2.0 inches. A horizontally oriented B-scan (i.e., parallel to the outer edge of the rib panel) is presented in Fig. 4.3. Similarly, a vertically oriented B-scan (i.e., perpendicular to the outer edge of the rib panel) is presented in Fig. 4.4. These figures both indicate the lateral extent of delamination, and also illustrate that the delaminations penetrate to approximately 0.2 inches from the indented surface of the composite.

4.2 Inspection of Areas of Interest Following 2P Loading

During the 2P pressure test case, some unexpected strain gage readings dictated that an inspection be performed of the crown panel end cap region centered between the frames. A B-scan from one of these inspections is presented in Fig 4.5. By comparison with the design drawing, in the lower panel, the strong back surface echoes can be identified as the number of fiber stacks is varied across the end cap flange. Also obvious is the ultrasonic "shadow" cast by the noodle material. To the inner side of the noodle appear several indications, apparently arising from delaminations in the stacks which form the curve of the inner corner of the end cap. Because of the shadow from the noodle, the only visible portions of the delaminations are those which extend beyond the arm of the noodle.

The occurrence of delaminations at this location was reasonable, given that pressurization of the cube would tend to open up the interior angle at the corner. This leads to stresses, which operate to separate the laminae in the corner.

Inspections were done on the central areas of all four edges of the crown panel, indicated by the dashed boxes in Fig. 4.6. Corner delaminations were observed on the opposite sides, between the frames, as indicated by yellow boxes in the figure, and were measured over 13 inches on each of these sides. Because of the shadow cast by the noodle, however, it could not be determined how far into the corner the delaminations extended. Furthermore, the interior surface of the corner was inaccessible for direct inspection because of sealant.

4.3 Post-Failure

In the final phase of testing, the PRSEUS cube was taken to higher pressure to induce structural failure. At a pressure of above 48 psi, failure occurred, resulting that the front bulkhead panel separated from the cube and was destroyed. The remaining panels remained attached to each other. A number of areas on the remaining cube panels were selected for ultrasonic inspection.

4.3.1 Three Types of Damage Identified

In analyzing the ultrasonic measurements of the cube after the test to failure, there were three distinct types of flaws identified. These three types are schematically depicted in Fig. 4.7. These types are defined as follows:

Type A: Delaminations between essentially flat laminae, most typically between the skin stacks and the stacks making up the flanges of stiffeners or end caps. There were also some Type A delaminations observed between tear strap stacks and the adjacent flange laminae. Two examples of Type A delaminations are shown in Fig. 4.8. Here, the unsupported flange tips

delaminated at the skin back surface. The delaminations terminated at the first row of stitches encountered under the stringer flange. In the end cap flange, the delamination extended past two stitch rows, before terminating at the third stitch row encountered. As will be discussed below, this particular end cap is the one to which the failed forward bulkhead had been attached.

Type B: Some delaminations were observed to occur in the laminae lying above the noodles of both stringers and frames. These occurred between the stitch rows on either side of the noodle. Fig. 4.9 presents two examples of stringers containing Type B delaminations. Fig. 4.10 presents the occurrence of Type B delaminations at several different levels in the end of a crown frame. Depths of the delaminated areas from the surface are identified (in inches) in the figure.

Type C: The corner delaminations, previously described as having been observed following the 2P test, are called Type C. These were observed in the interior fillet laminae of the end caps. Examples of Type C flaws are depicted in Fig. 4.5 (after 2P test) and in Fig. 4.9 (after test to failure).

4.3.2 Crown Panel

The results of inspection of the crown panel are presented in Fig. 4.11. Different colored areas indicate the three types of damage: Type A in blue, Type B in orange and Type C in yellow.

Only a small amount of flange delamination (Type A) was observed. Two areas were found adjacent to the end cap and central stringer along the connection with the failed bulkhead panel. A third area was observed at the first stringer and frame intersection. This is near the location proposed as the initiation site of ultimate failure: the metallic splice plates connecting the crown and rib frames [2, 4].

Type B delaminations were observed on all the stringers, between the frames. Patches of Type B flaws were observed at several depths in all the frames, typical of those presented in Fig. 4.10, near the corners where the frame intersects the end cap and stringer.

Type C corner delaminations were observed over approximately 2/3 of the length of the end caps. Because these results only include those parts of the fillet delaminations which extend beyond the limb of the noodle cross-section, some unknown amount of Type C damage might have gone undetected during these inspections.

4.3.3 Right Rib Panel with Impact

Figure 4.12 presents a summary of results obtained for the right rib panel containing the impact site. The area inspected includes the forward end cap, the vertical structure on the right hand side containing the BVID impact and to which the failed bulkhead panel had been attached, and the vertically-oriented rib frame. The uppermost part of the scan includes the interface with the crown panel, and the seven stringers are horizontal.

There were no observable changes in the damage surrounding the BVID impact site.

Type A delaminations were found along the end cap flange at each bay. These were at the level of the face sheet stacks, and fell within the area of the unsupported flange ends, terminating at the first row of stitches. A much larger area of delamination was found in the upper right corner of the panel, near the intersection of the rib frame with the crown frame, the suspected initiation site for the ultimate failure.

Delaminations of Type A were observed in the flange of the rib frame, at each bay scanned. These fell at the level between the tear strap and the frame flange laminae.

Type B delaminations were found in each of the stringers scanned in the central area of the panel, between the frames.

Lengths of Type C delaminations were observed along the uppermost stringer, between the frames, and along the central span of end cap adjacent to the Aft Bulkhead.

4.3.4 Left Rib Panel

A summary of inspection results for the Left Rib Panel is given in Fig. 4.13. Type B delaminations were found in the stringers between the frames. Type C indications were observed in the central length of the bottom cap.

4.3.5 Aft Bulkhead Panel

The inspection of the Aft Bulkhead is summarized in Fig. 4.14. Type B delaminations were identified in the bottom cap and in stringers between the vertical frames. Small areas of Type A and Type B delaminations were found in the frames, with notable symmetry in the size, shape and locations of the flaws.

4.4 Inspection of Cutout Sections

After the post-failure ultrasonic inspections were completed, the remains of the cube test article were shipped from NASA LaRC back to Boeing for further analysis and dissection. Because the first indications of material damage appeared during the 2P test in the Crown Panel end caps near the midline between frames, a more detailed inspection of this material was requested, to involve immersion ultrasonic and x-ray computed tomography to be performed at NASA LaRC.

4.4.1 Description of cutout sections

Two sections of the crown end caps were dissected for analysis. Figure 4.15 indicates these areas by blue rectangles. The specimens were labeled Side A and Side B. Because the crown panel had been spray painted after the installation of strain gages and wiring, there was a clearly identifiable pattern on the two specimens where the gages, wiring and tape had been removed. These marks aided in identifying the precise locations of the two specimens on the crown panel. Photographs of specimen Side A and its location on the crown panel are compared in Fig. 4.16.

Examination of the end of the specimens is useful. In Fig. 4.17 an ultrasonic B-scan from this region, taken following the 2P load test (see Fig. 4.5), is overlaid onto a photograph of the end of specimen Side A. Some of the stitches are readily identifiable in the photograph; orange lines indicate others.

The broad, echo-free area in the B-scan is observed to correspond well to the crown edge of the “triangularly-shaped” noodle region, which was filled with a low density of bundled fibers during fabrication.

4.4.2 Ultrasonic inspection of cutout sections

Immersion ultrasonic data were acquired using a 10 MHz, 0.5-inch diameter, and 2.0-inch focal length spherically focused immersion transducer. A C-scan acquired with the beam incident

normal to the outer surface of specimen Side A is presented in Fig. 4.18 along with a photograph of the front surface for comparison. The C-scan data represents scattering from just beneath the surface of the part. At this level, the ultrasonic signal has clear disturbances corresponding to the stitching material at that surface. Colored dashed lines are used on the figure to indicate these stitch rows. The (nominally) vertically oriented stitch rows are in yellow, while the angled stitches are in red or orange, depending on the direction of the diagonal.

A B-scan through the specimens (like that in Fig. 4.17, but flipped horizontally) is shown in Fig. 4.19. Along the line of the echo arising from the front surface of the part, colored dots are used to indicate the positions of the stitch entry points on that surface, as shown on the C-scan in Fig. 4.18. Corresponding locations were identified for the exit points of the stitches on the back surface of the specimen by manipulating the grayscale representation of the data. These points are indicated by colored dots on the back surface echoes in Fig. 4.19. Connecting corresponding entry and exit dots with colored dashed lines indicates the approximate location of the stitch material in the volume of the composite.

A significant observation from this figure is that the ultrasonic echoes arising from Type C delaminations occur in the volume between the diagonal stitch adjacent to the noodle and the matching vertical stitch. On the noodle side of the diagonal stitch, ultrasonic echoes fade away into the echo-free zone.

Secondly, the extent of the very nearly echo-free area falls close to the diagonal stitch on either side of the noodle, which is not all in the geometrical shadow of the noodle material.

Figure 4.20 combines the B-scan from Fig. 4.19 (rotated 90° counterclockwise) with a C-scan of the specimen representing the peak echo amplitude from the interior of the specimen. The white dashed lines on the B-scan indicate the depth gate. The Type C delaminations are observed to extend the entire length of the specimen, and to be contained between the red stitch row and the adjacent yellow stitch row.

The end cap itself was also scanned. Figure 4.21 presents a C-scan and two B-scans of the cap. Again, on the C-scan, vertically oriented stitch rows are indicated by dashed yellow lines. A solid red line and a solid orange line indicate the locations of the B-scans presented in the figure. These fall in the area containing Type C delaminations adjacent to the internal fillet, and between two rows of stitches where no delamination indications are observed.

The Type C delaminations fall in the area between the first row of stitches at the fillet (out of the data region at the top of the scan) and the second row of stitches.

4.4.3 X-ray Computed Tomography (CT) of cut-out sections

A 1.5-inch long portion of the specimen Side A was imaged using high-resolution x-ray computed tomography (CT), with a voxel resolution of approximately 20 microns (0.0008 inch). A section of this data across the noodle and inner fillet region of the specimen, including one diagonal stitch, is presented in Fig. 4.22.

One general observation of the CT data is that the composite has few voids or resin-starved areas, indicating a successful infusion of resin into the dry preform.

Also quite prominent is the relatively resin-rich noodle volume. Some degree of voids and cracking are observed in the noodle volume, predominantly within the resin.

The interior fillet laminae are observed to be highly delaminated. It appears that the boundary between each pair of stacks (7-ply layers, held together by polymer knitting threads, stacked up to build the composite) is delaminated, causing an effect resembling the layering of an onion. These multilayer delaminations were observed to extend over the entire 1.5-inch length of the CT.

Almost all of the "onion-layer" delaminations in Fig. 4.22 end at the position of the diagonal stitch in the face sheet. Toward the end cap, the "onion-layer" delaminations end before or at the position of the first stitch row. At both ends of the curve, some small fraction of delaminations extends beyond the first stitches encountered. These are the portions of the delaminations found by ultrasonic inspection (Figs. 4.20 and 4.21), but all delaminations end before reaching the next row of stitching.

It is observed that some occasional small voids occur within or adjacent to the stitching threads. Some crack-like indications are observed along the boundary of the stitch threads and the surrounding composite, indicating thread separation from the composite during cure. These indications are not widespread, and their presence doesn not appear to affect the material behavior.

Figure 4.23 shows analysis results predicting high out-of-plane stresses in the inner fillet of the end cap, consistent with formation of the observed "onion-layer" delaminations. Interlaminar failures were predicted to occur at 12.4 psi, while the first indications of damage from strain gages occurred at approximately 16 psi during the 2P load test [4].

5.0 Discussion

Based on the results of ultrasonic and x-ray nondestructive testing, the PRSEUS system demonstrated damage contraint in this test. The damage from an intentional BVID site did not grow during applied load. The numerous delaminations that occurred within the structure at higher loads were almost completely contained by the first row of stitches. Where the delaminations did extend beyond the first stitch row, at all but two or three measured sites the delaminations ended before or at the second stitch row. Those few sites where two stitch rows were crossed were located adjacent to the failed bulkhead panel, and likely occurred during the last moments before catastrophic failure of the bulkhead [2].

One area of potential concern for nondestructive evaluation of PRSEUS is the behavior of the ultrasonic interrogation around the noodles. As illustrated by the B-scans in Figs. 4.5, 4.9, 4.17 and 4.19, the material in the noodles was highly attenuative and/or poorly backscattering to the ultrasonic signal. The physical reasons for this behavior were made apparent by the high-resolution of the CT cross-section of the noodle region.

The x-ray CT in Fig. 4.22 is reproduced in Fig. 5.1 to support this discussion. For all of the ultrasonic inspections from the outer surface of the cube, the ultrasonic beam was incident normal to the surface. The ultrasonic waves penetrating the face sheet are represented by the parallel vertical lines in the face sheet area in the figure.

The noodle volume is seen to be a much different consistency than the material in the face sheet. Bundles of fibers (oriented roughly perpendicular to the image) are loosely distributed in the volume surrounded by resin matrix fill material. For reference, the approximate size of a 10 MHz wavelength is displayed in white. Because the ultrasonic velocity in the resin is quite different than that in the fiber bundles, this noodle material exhibits ultrasonic velocity discontinuities which are on the order of several wavelengths in dimension, resulting in scattering

and refractive phenomena which disperse the ultrasonic beam, with the result that little or no ultrasound is sent back in the direction of the transducer, causing an echo-free zone. The yellow arrows in Fig. 5.1 illustrate this behavior.

Further analysis of the structure suggests that another phenomenon, related to the curvature in the fillet laminae, is also acting in this case. The orange arrows in Fig. 5.1 illustrate the normal-incidence ultrasonic waves propagating through the face sheet laminae into the parallel laminae of the end cap flange, beyond the first row of stitches from the end cap. Here, the ultrasonic waves encounter a delamination which has extended beyond the stitch row. This delamination is parallel to the interlaminar interface and perpendicular to the incident wave propagation, so the ultrasound is reflected from the delamination back to the transducer to be detected. These represent the delamination indications labeled Type C.

However, on the end cap side of the diagonal stitch row, the fillet laminae curve away from the flat face sheet laminae, and because of the thickness of the inner fillet, this curvature extends laterally away from the direct "shadow" of the "triangular" noodle volume. This enables a different refraction behavior to occur.

Fiber-reinforced plastic composites exhibit anisotropic ultrasonic characteristics. The ultrasonic velocity is much faster for propagation in the direction of fibers than it is across the fibers. In a quasi-isotropic laminate, such as the stacks used in PRSEUS, the result is that the ultrasonic velocity is higher in the plane of the stack than normal to the plane. So, in the case presented in this region, the ultrasonic waves propagating normal to the laminae in the face sheet, then encounter laminae which are curving away from the plane. This causes the ultrasonic waves to deviate their path, due to refraction, toward the direction of faster ultrasonic velocity, i.e., toward the direction of the curving laminae. As illustrated by the red arrows in Fig. 5.1, these refracted waves divert away from a path which results in reflections back toward the transducer, leading to an effective widening of the echo-free zone, as best illustrated in Fig. 4.19.

6.0 Conclusions

It was observed that the damage incurred within the PRSEUS pressure cube during this series of mechanical tests was contained by the stitches.

It was also found that the construction of the noodles used in the PRSEUS Pressure Cube prevented a full ultrasonic inspection of the highly-stressed inner fillet of the integral caps.

7.0 References

1. Boeing Document ZA153690, Pressure Cube Test Specification, (2011).

2. Andrew E. Lovejoy, "PRSEUS Pressure Cube Test Data and Response," NASA TM-2013-217795.

3. Michael R. Horne, "Evaluation of Acoustic Emission SHM of PRSEUS Composite Pressure Cube Tests," NASA TM-2013-217993.

4. Nicolette Yovanof, Andrew E. Lovejoy, Jaime Baraja and Kevin Gould, "Design, Analysis and Testing of a PRSEUS Pressure Cube to Investigate Assembly Joints," 3rd Annual Aircraft Airworthiness and Sustainment Conference, Baltimore, MD, April, 2012.

5. A. Velicki, "Damage Arresting Composites for Shaped Vehicles," NASA-CR-2009-215932, (2009).

6. D. Jegley, “Experimental Behavior of Fatigued Single Stiffener PRSEUS Specimens,” NASA-TM-2009-215955, (2009).

7. Patrick H. Johnston, “Pulse-Echo Phased Array Ultrasonic Inspection of Pultruded Rod Stitched Efficient Unitized Structure (PRSEUS),” Review of Progress in Quantitative Nondestructive Evaluation, vol 30, AIP Conf. Proc. 1335, pp. 1432-1439 (2011).

TABLE 1. Load Sequence

Load Sequence	Load Set	Instructions	Comments
0	0.5P (4.6 psi)	Instrumentation checkout. Verify that all instrumentation is working and being recorded	Instrumentation should be completed prior to Boeing's arrival for test witnessing
1	1.33 P (12.2 psi)	Build pressure to 0.5P, 1P & 1.15P stabilizing at each level. Then build up to test pressure of 1.33 psi. Hold pressure at 1.33 psi for 3 seconds, then depressurize.	The panel is pressurized to gather linear data. The data will be used to calibrate with analysis.
2	2P (18.4 psi)	Build pressure to 1.33P and stabilize. Then build up to test pressure of 2P. Hold pressure at 2P for 3 seconds, then increase to 2P + 10% and hold for 3 seconds, then depressurize.	Check 1.33P panel characteristics for linear behaviors. The panel will then be loaded up to 2P under pristine condition. The test will verify the capacity of minimum gage skin design with integral caps as joints
3	Damage Panel	The panel shall be impacted with BVID as described in Section 2.3 prior to testing to failure. The panel shall be inspected using NDI before and after impacting at the damage location with a radius of 4 inches from the edge of the damage.	In order to demonstrate the capability of the joint under BVID with 100 ft-lb impact damage on the skin side of the rib panel and the radius of the integral cap, the panel will be damaged prior to failure.
4	To Failure	Build pressure to 1.33 P and stabilize. Build pressure to 2P and stabilize, hold for 3 seconds. Then build pressure to failure.	The impacted panel will be pressurized until failure. The test will verify the ultimate capacities of the panel in pristine condition.

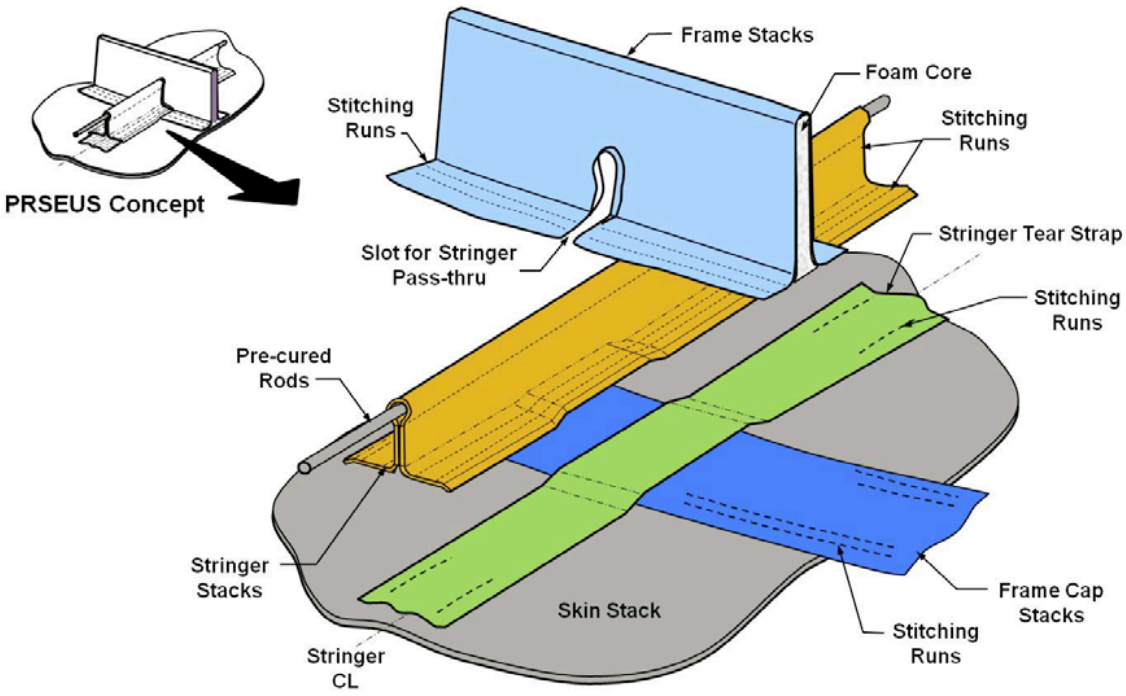

Figure 2.1. The PRSEUS dry preform is built up from carbon fabric stacks for the frame, stringers and skin. The layers are stitched together with Vectran fibers, using a single-sided sewing method, then bagged and infused with resin [4].

Figure 2.2. An example of a PRSEUS panel. This particular flat panel comprises four frames and seven stringers [5].

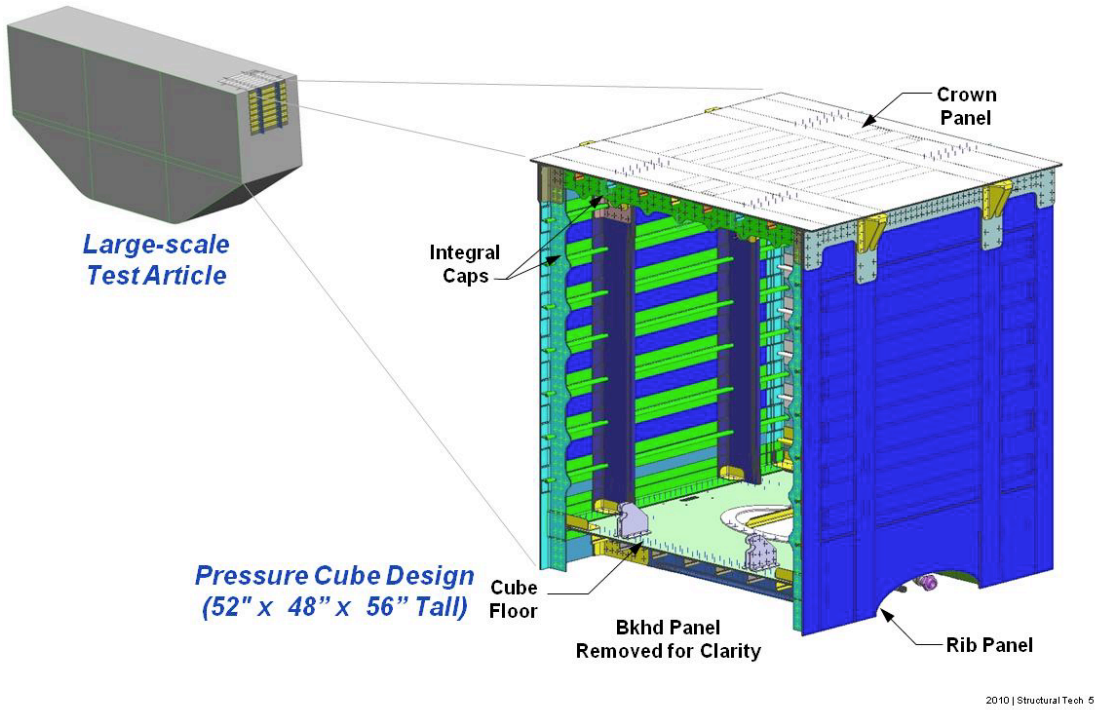

Figure 2.3. Test specimen assembly, representing a portion of the large-scale multi-bay test article.

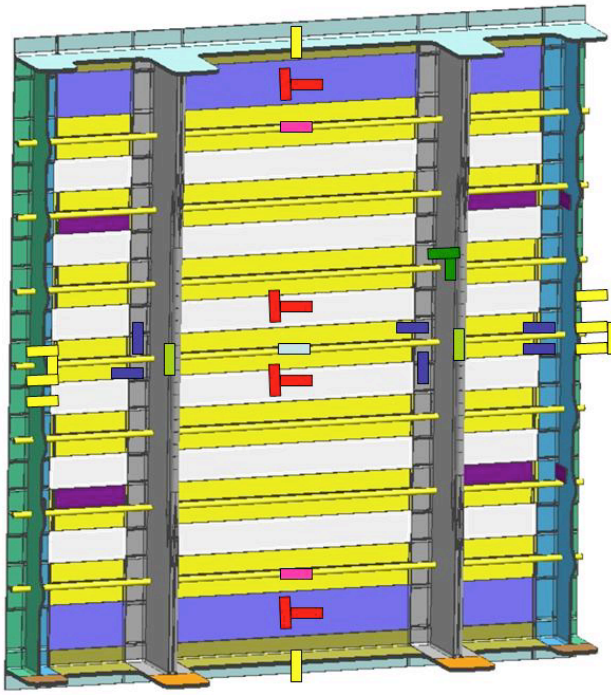

Figure 2.4. Crown panel, comprising two frames, seven stringers and end caps along all four edges

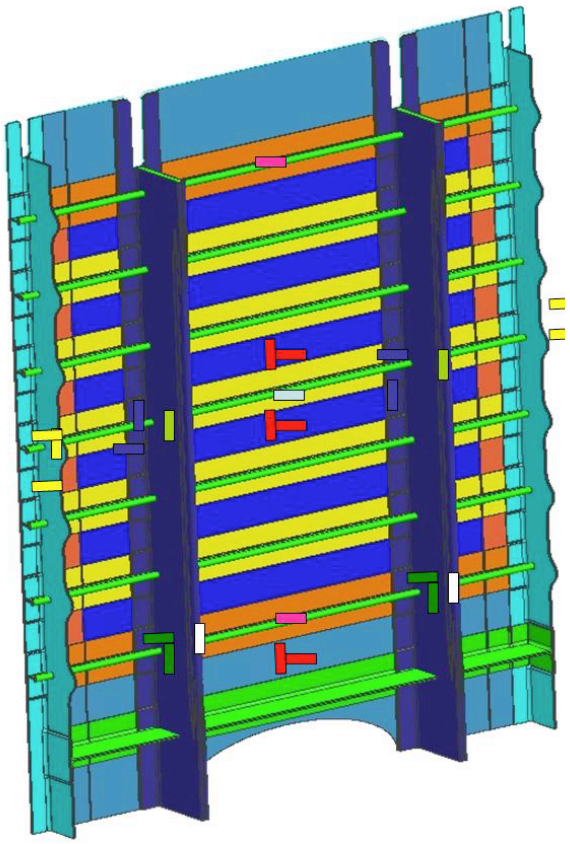

Figure 2.5. Rib panel, comprising two frames, seven stringers and end caps on vertical edges and bottom edge.

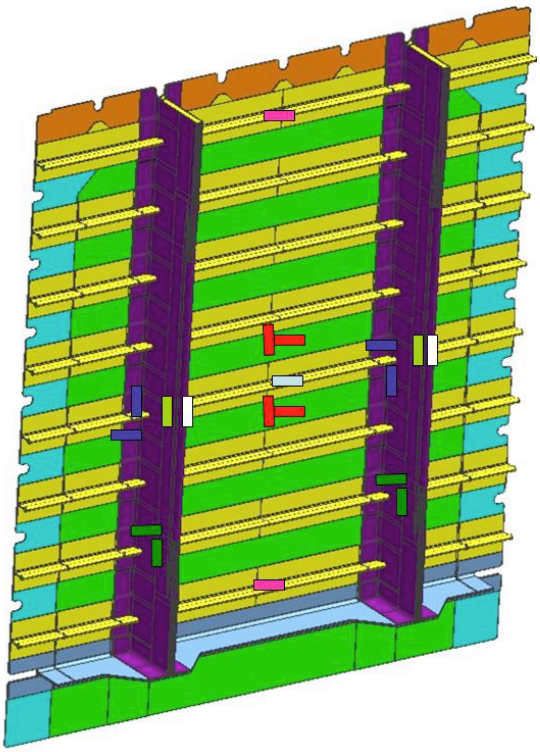

Figure 2.6. Bulkhead panel, comprising two frames, eight stringers and an end cap on the bottom edge.

Figure 3.1. A linear ultrasonic array attached to a manual X-Y encoder was used to interrogate the PRSEUS panel. Ultrasonic coupling was accomplished using a plastic wedge and soapy water.

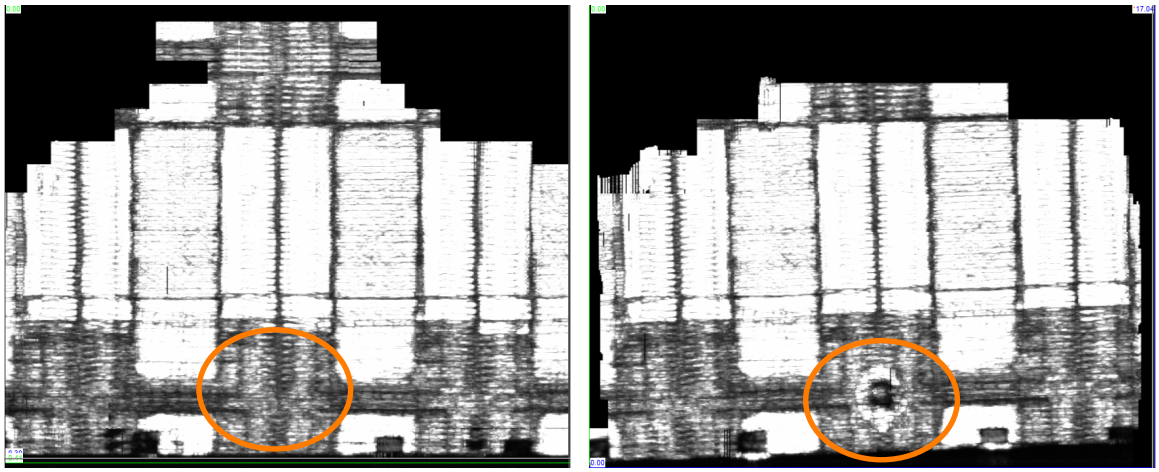

Figure 4.1. Ultrasonic C-scan results from the site of impact before (left) and after (right) the impact was performed.

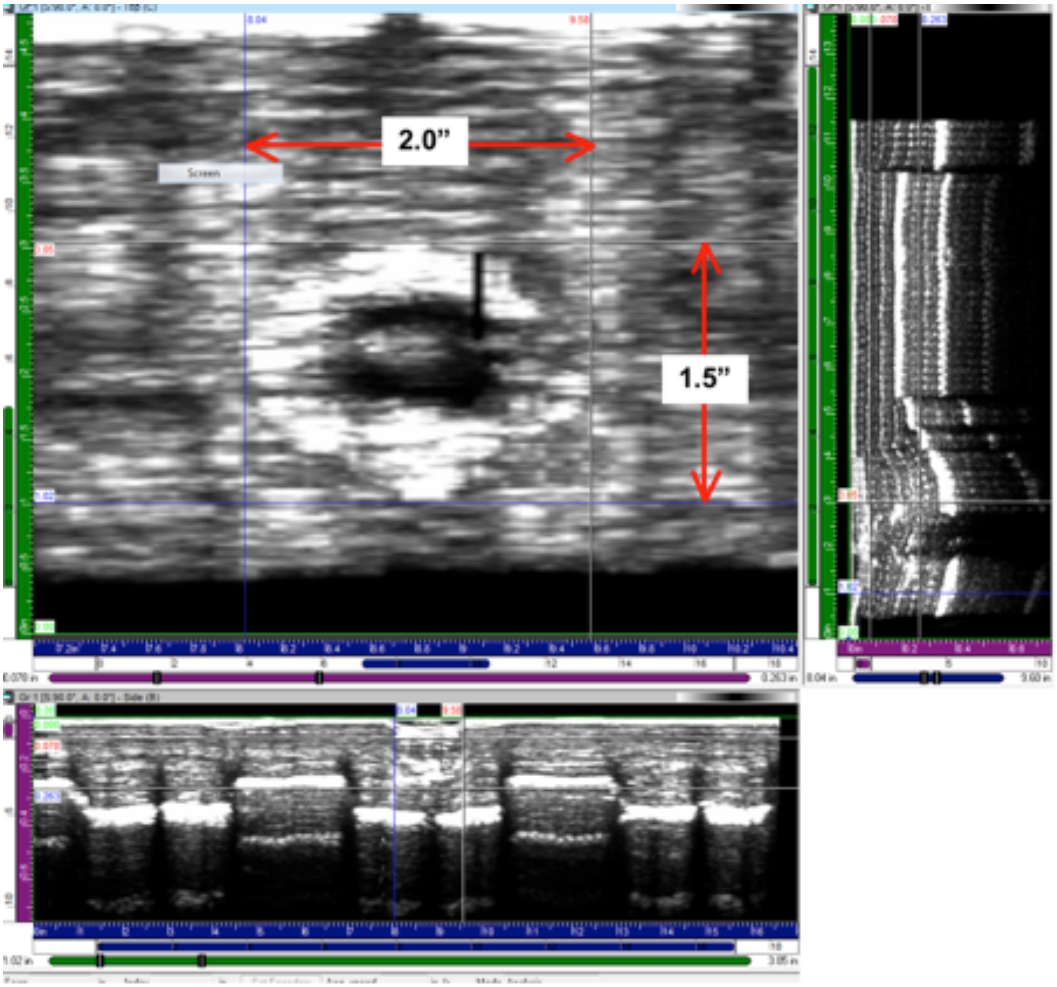

Figure 4.2. Close-up C-scan of the impact site (upper left) with vertically oriented B-scan (right) and horizontally oriented B-scan (bottom).

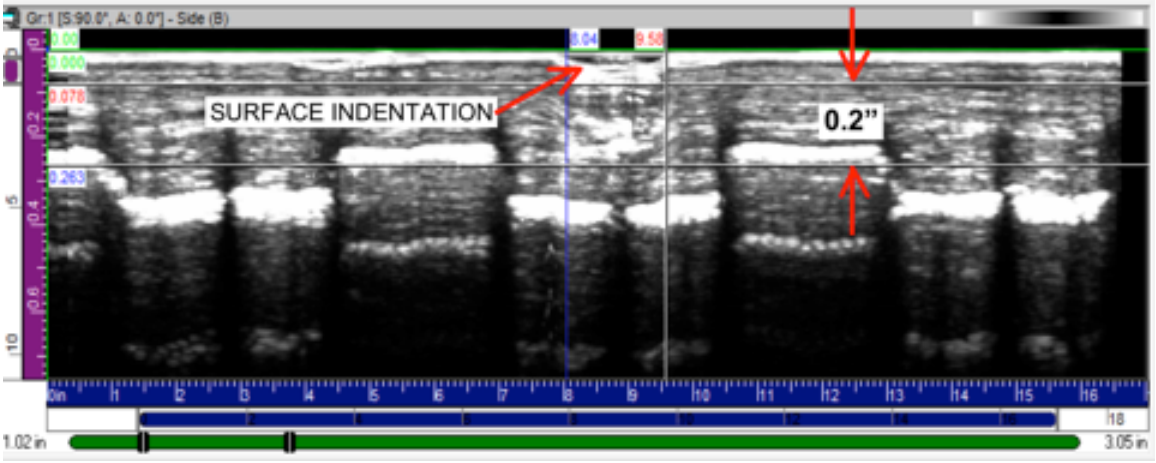

Figure 4.3. Horizontally oriented B-scan through the impact site, highlighting the indentation of the surface and indicating the depth of impact-generated delamination damage.

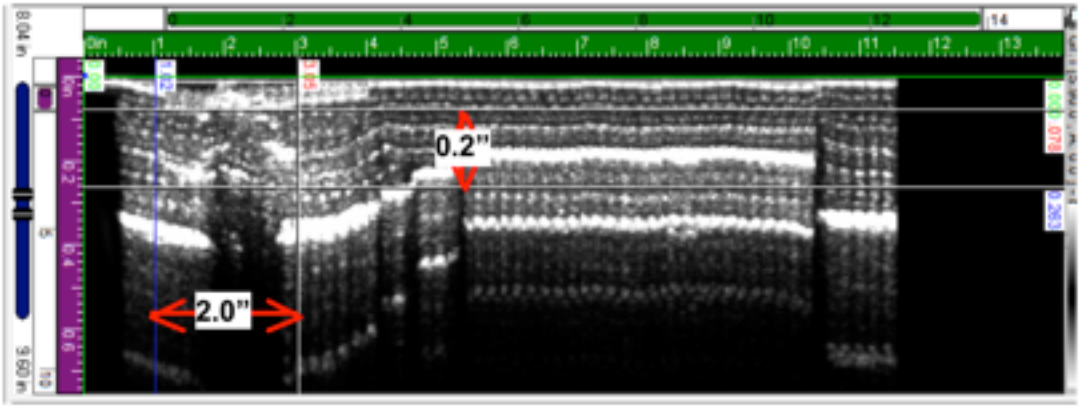

Figure 4.4. Vertically oriented B-scan through the impact site, indicating the width and depth of impact-generated delamination damage.

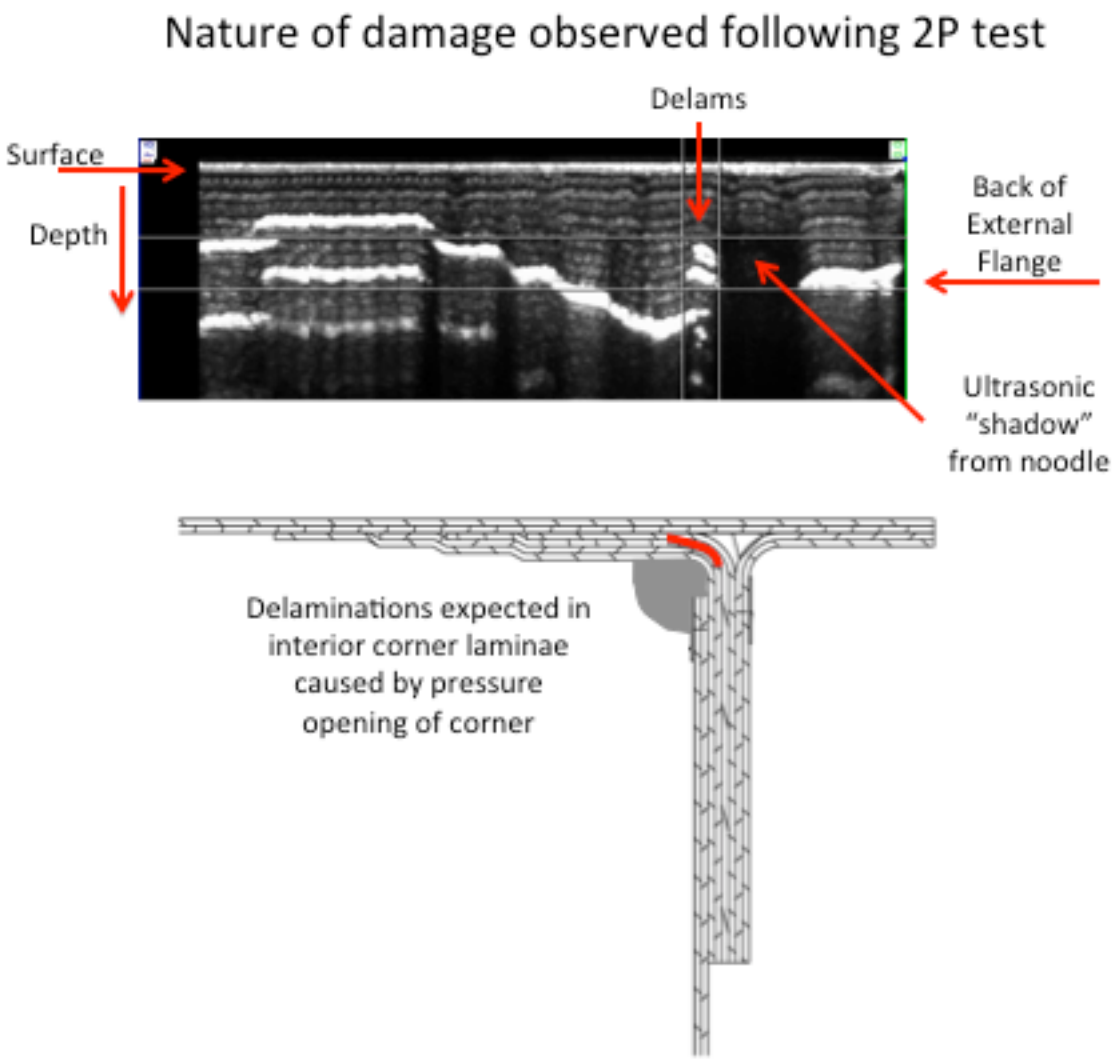

Figure 4.5. Ultrasonic scans were taken following anomalous strain gage readings during the 2P pressurization test. Notice the ultrasonic shadow cast by the highly-attenuative noodle material. It is likely that the delaminations extend further along the curve of the laminae, but are hidden from the inspection by the width of the noodle.

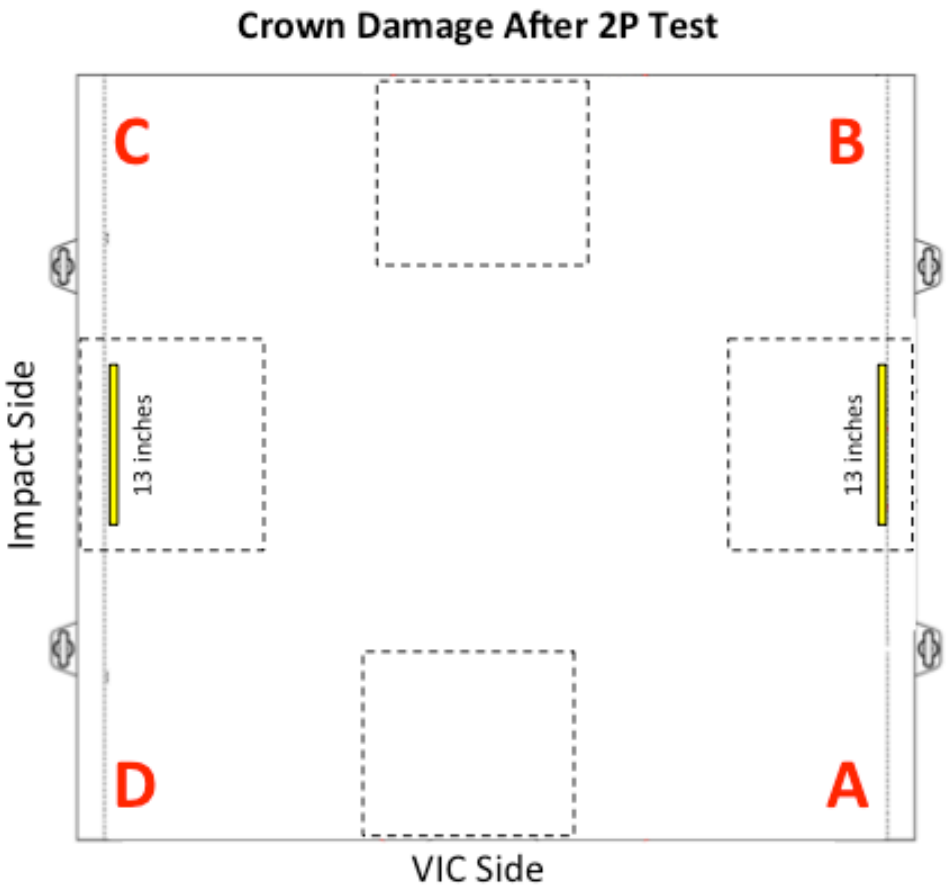

Figure 4.6. Summary of the crown panel damage observed following the 2P pressure test. Delaminations were observed adjacent to both end caps, at middle of crown panel, between the frames. The observable portion of the delaminations extended approximately 13 inches in length.

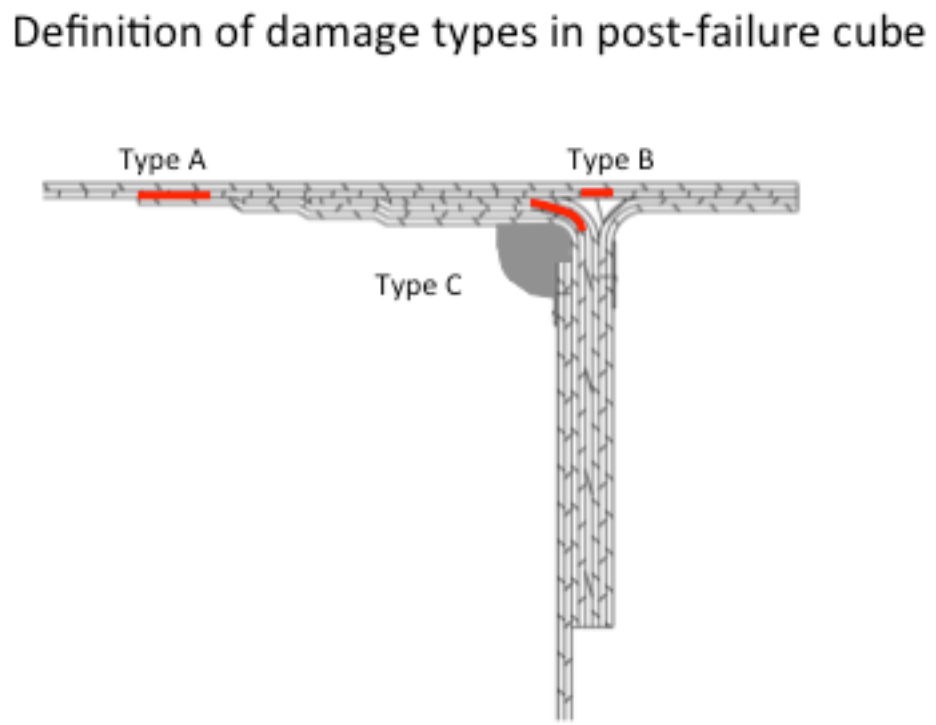

Figure 4.7. Definition of damage types found in cube following test to failure. Type A is a delamination between the skin laminae and the laminae comprising the flange of a stringer, frame or end cap. Type B is a delamination in the laminae above the noodle of a stringer, frame or end cap. Type C delaminations occur in the curved laminae forming the inner corner of an end cap.

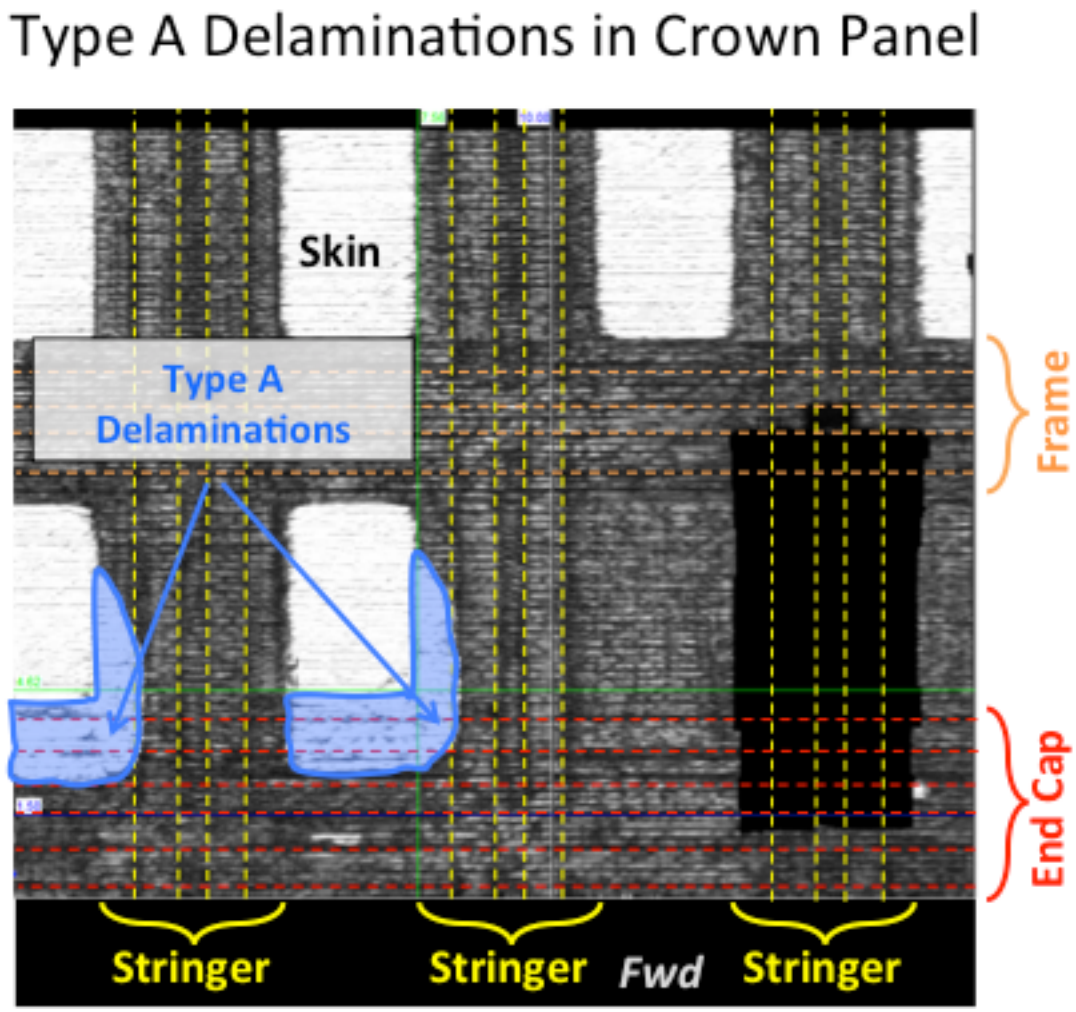

Figure 4.8. Example of a Type A delamination, which is an extension of the inner skin surface underneath the stringer flange laminae.

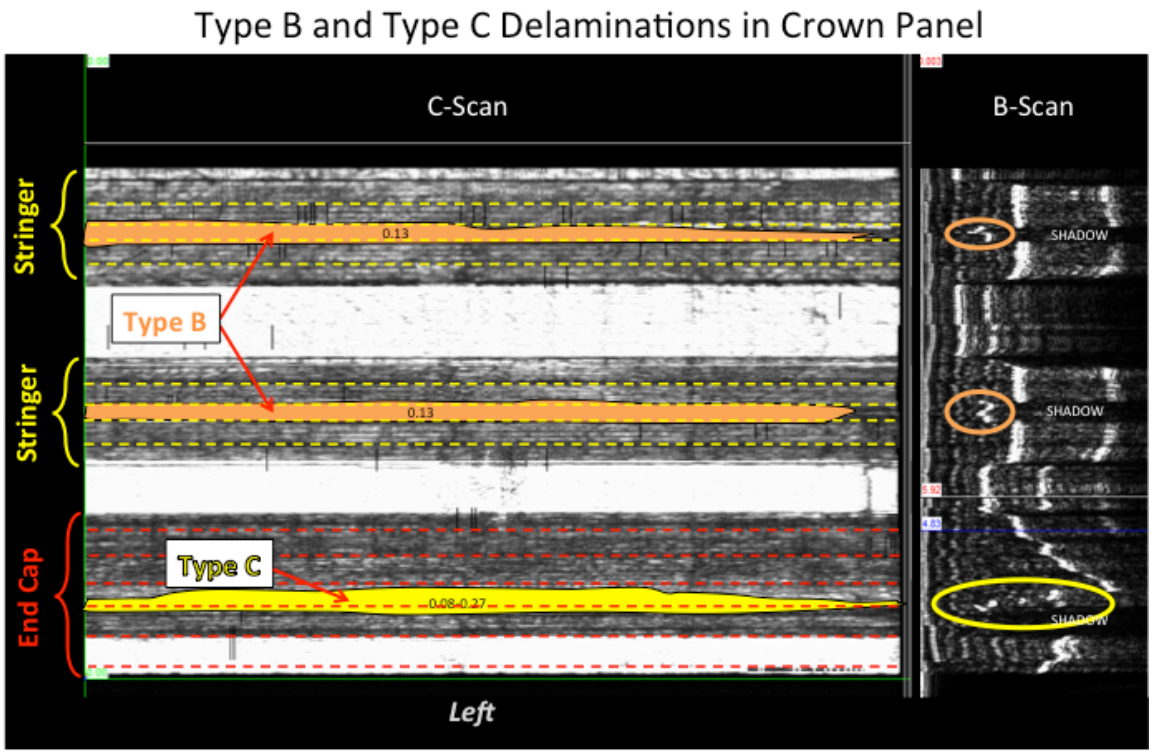

Figure 4.9. Example of a Type B and Type C delaminations Type B damage is seen above the noodle of two stringers. Type C damage is observed to the side of the noodle of the end cap.

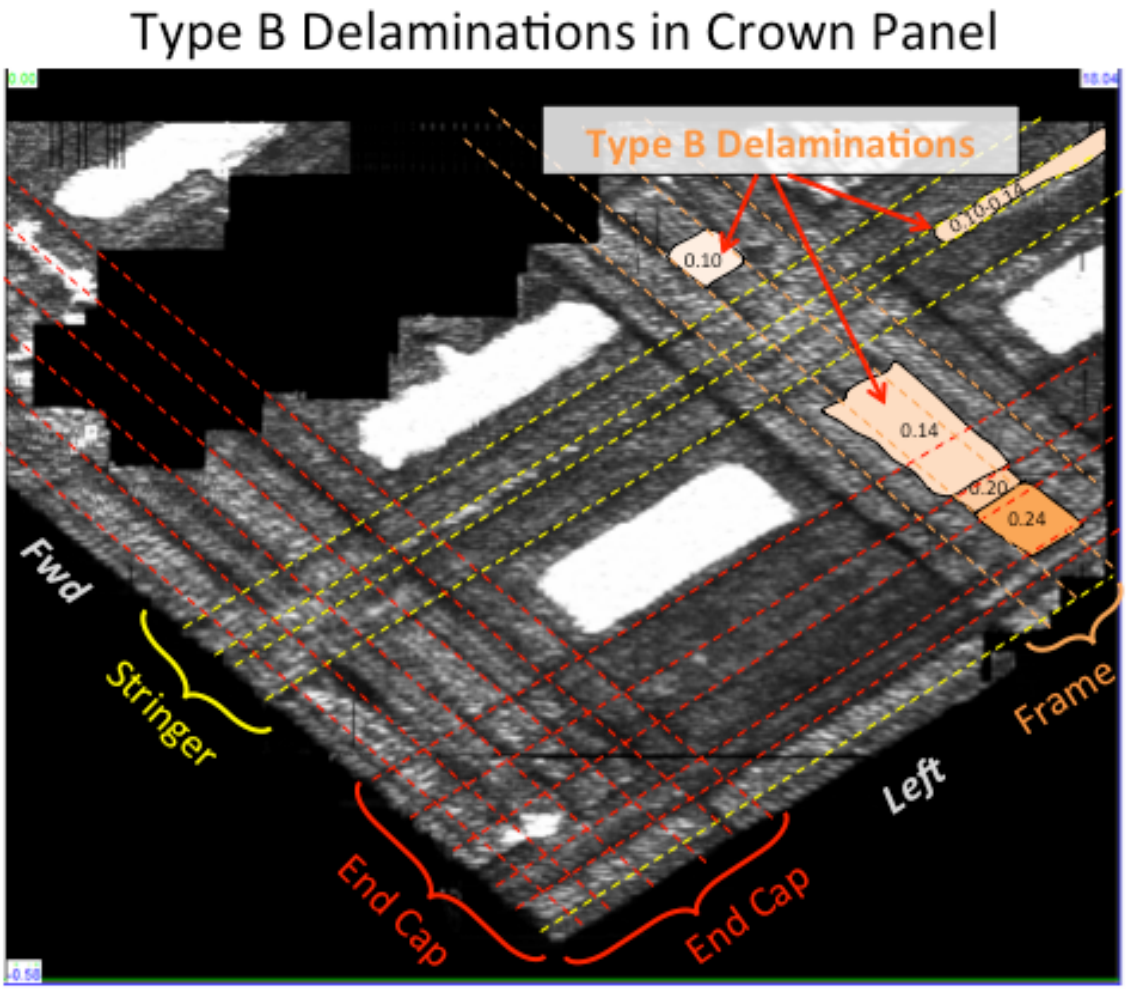

Figure 4.10. An example of Type B delaminations above the noodle of a frame.

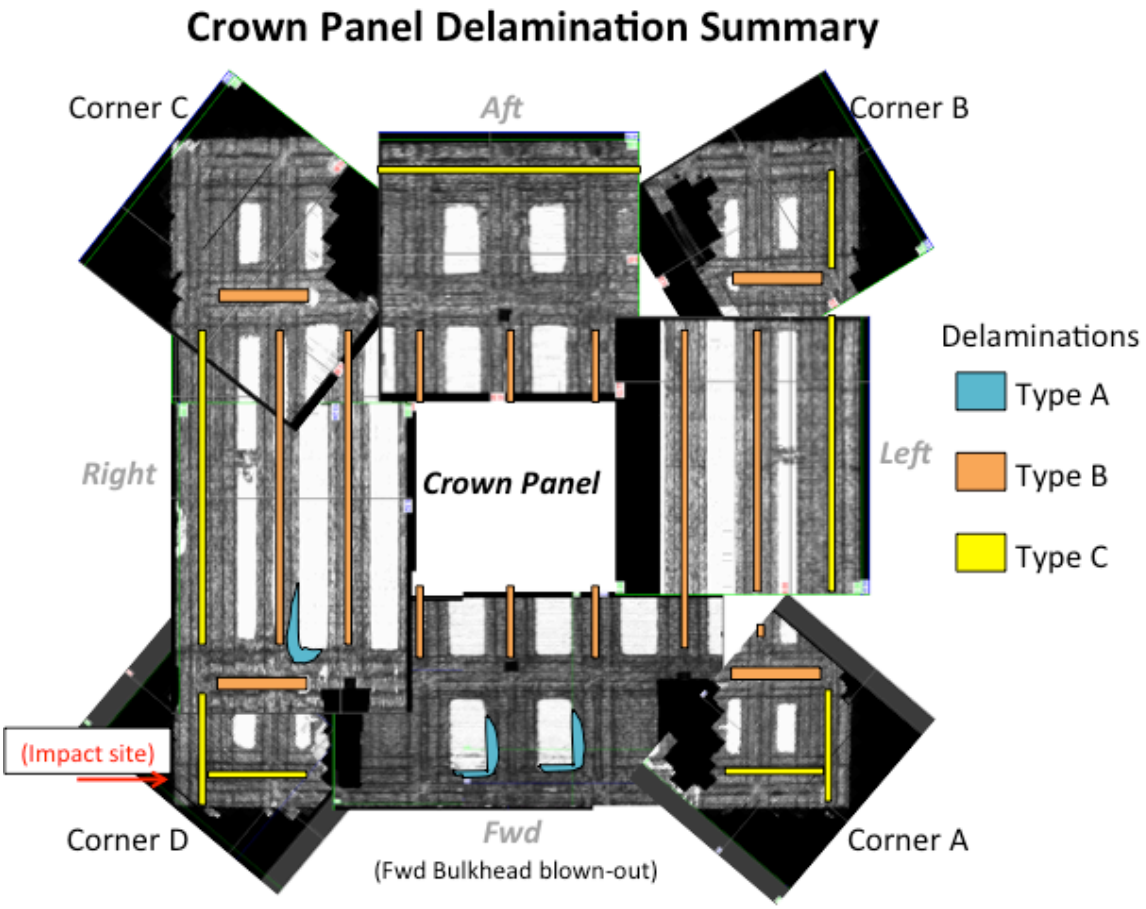

Figure 4.11. Summary of the post-failure damage observed in the Crown panel.

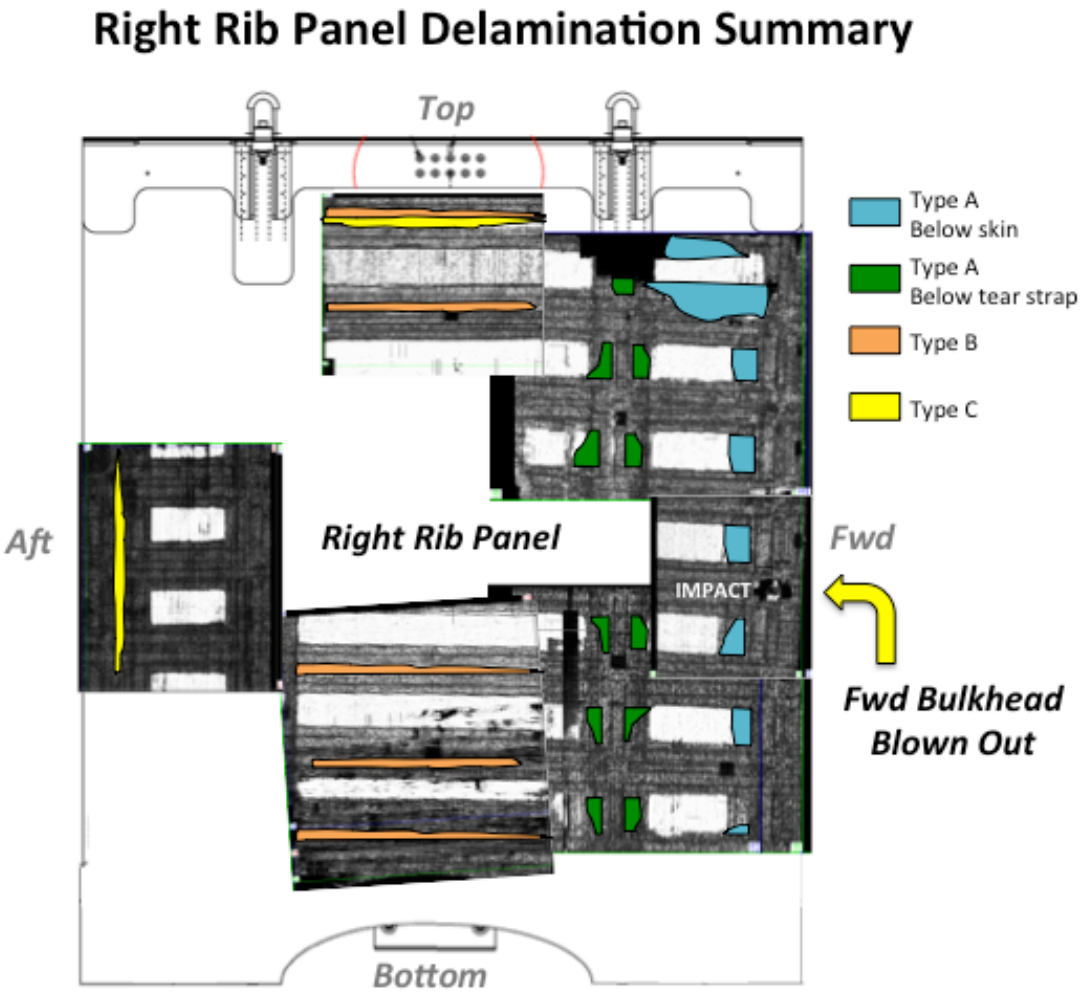

Figure 4.12. Summary of the post-failure damage in the Right Rib panel containing the impact site.

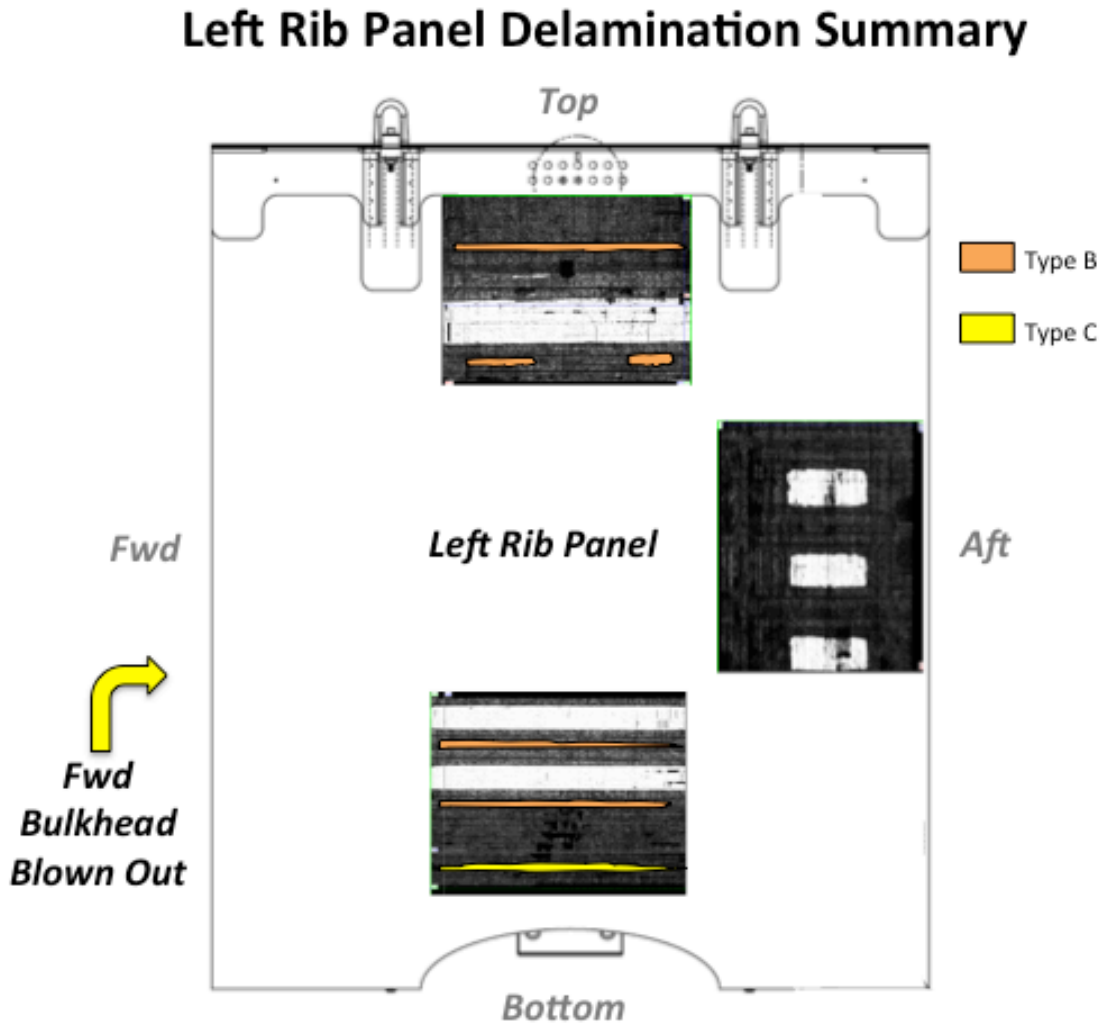

Figure 4.13. Summary of the post-failure damage in the Left Rib panel.

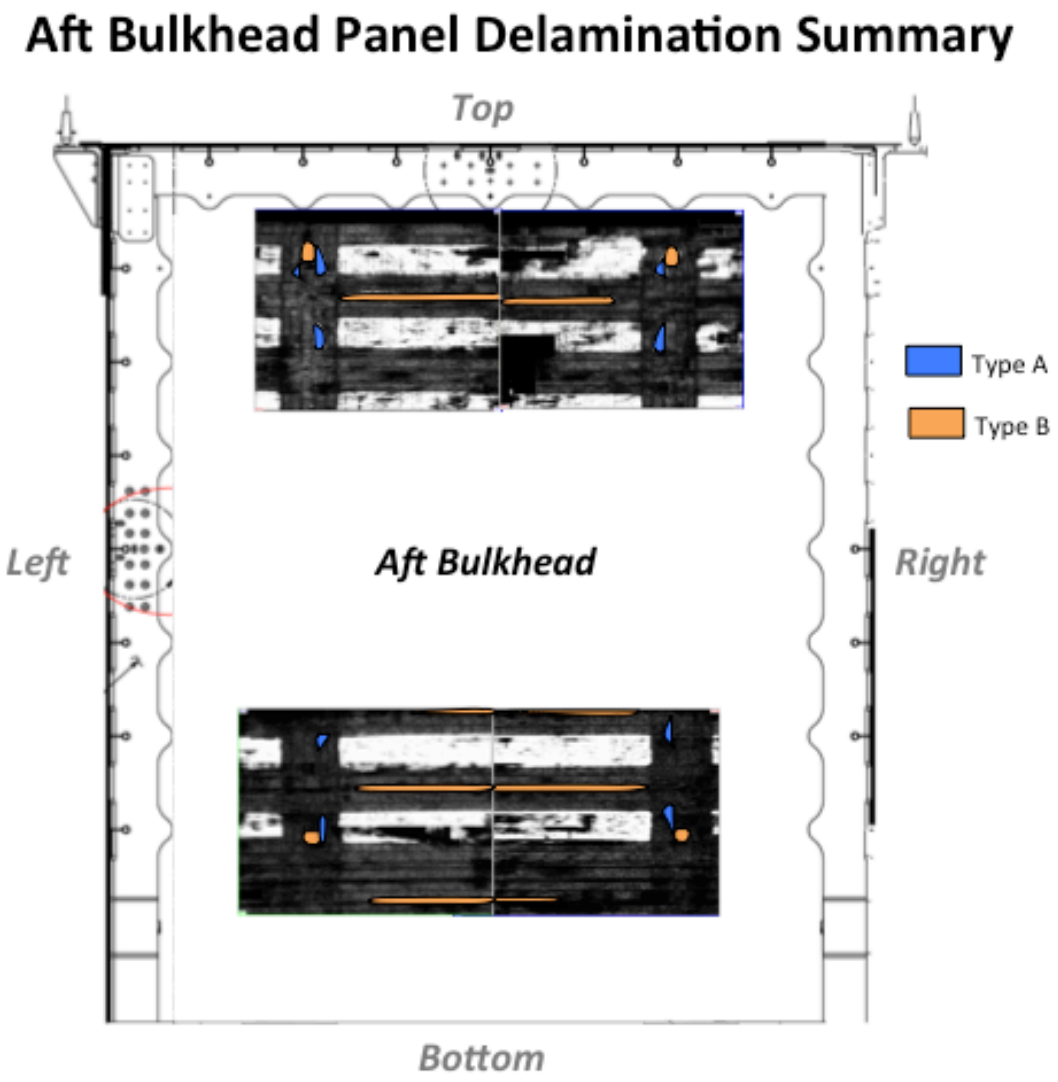

Figure 4.14. Summary of the post-failure damage in the Aft Bulkhead panel.

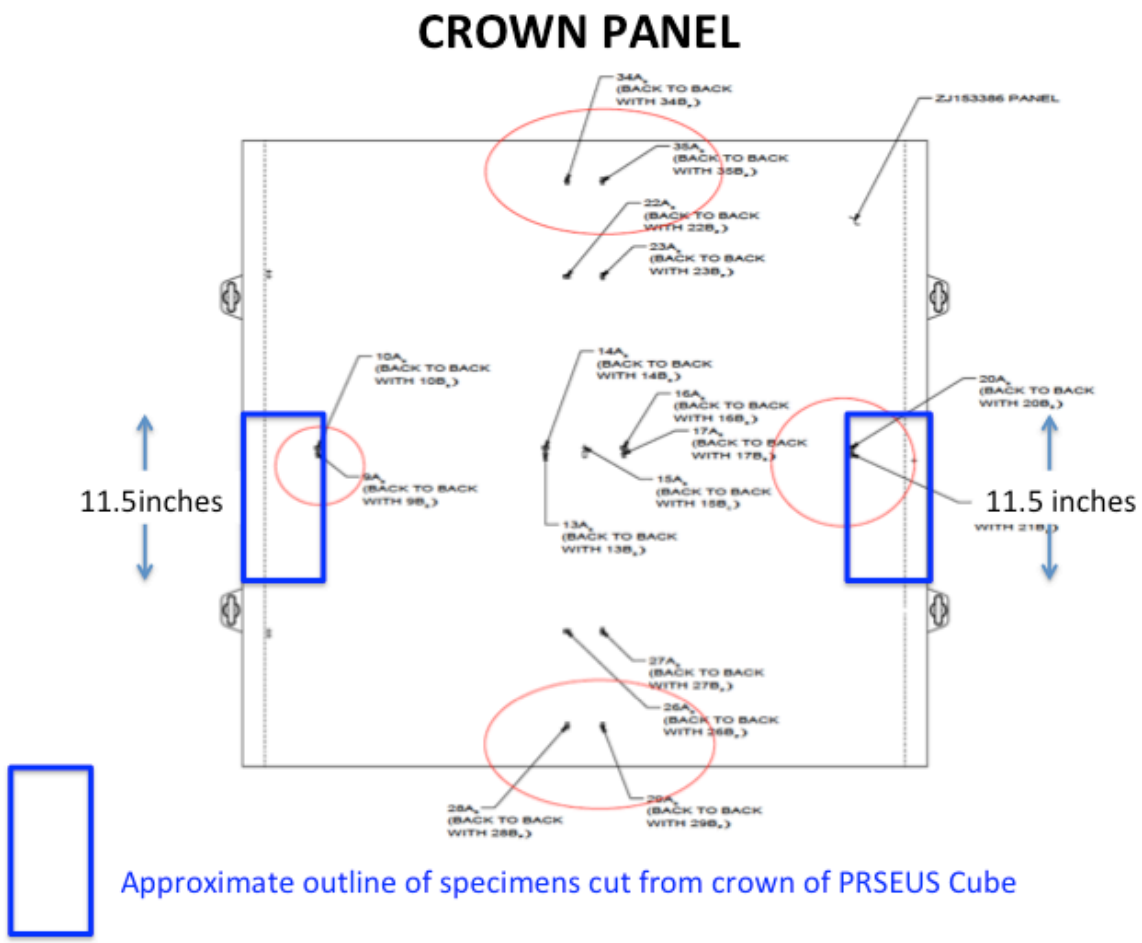

Figure 4.15. Areas of Crown panel selected for cutout and further inspection

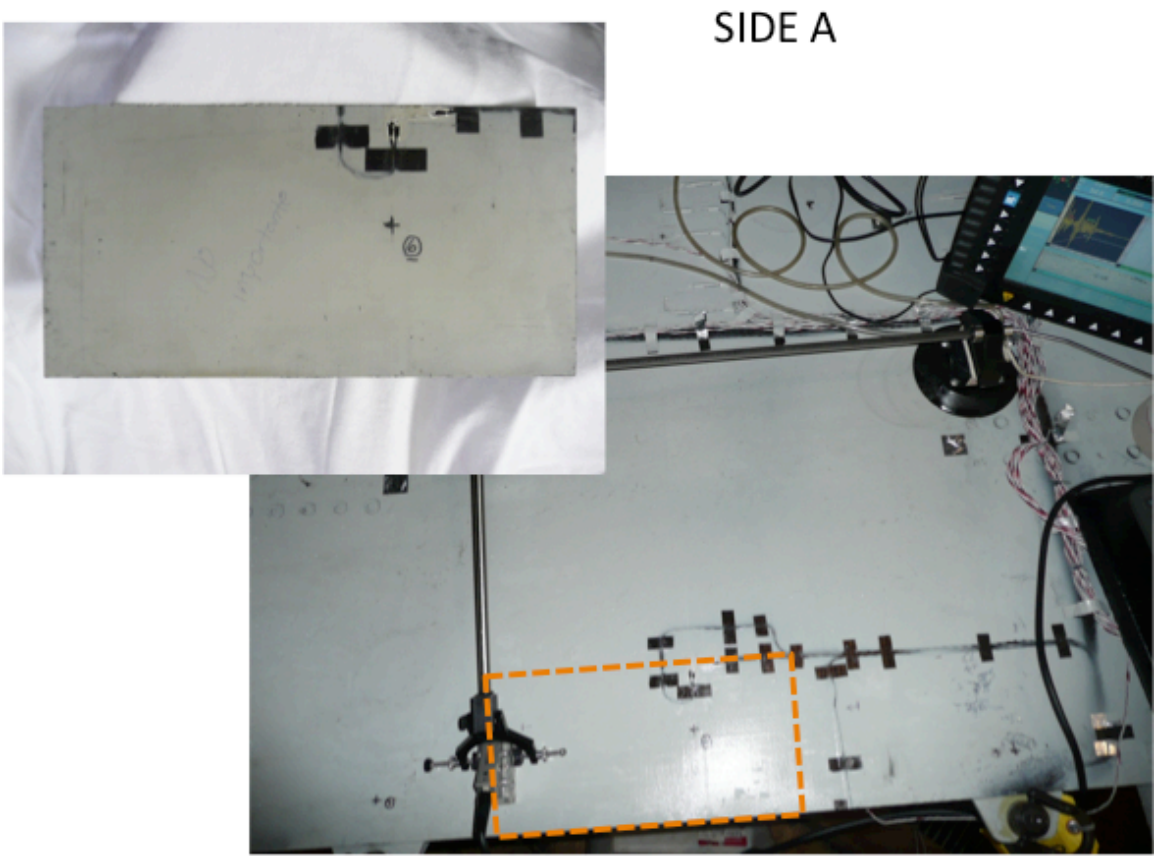

Figure 4.16. Photograph of the external surface of cutout labeled Side A. Below is a photograph of the intact crown under inspection, with the extent of Cut-out Side A identified by an orange dashed rectangle.

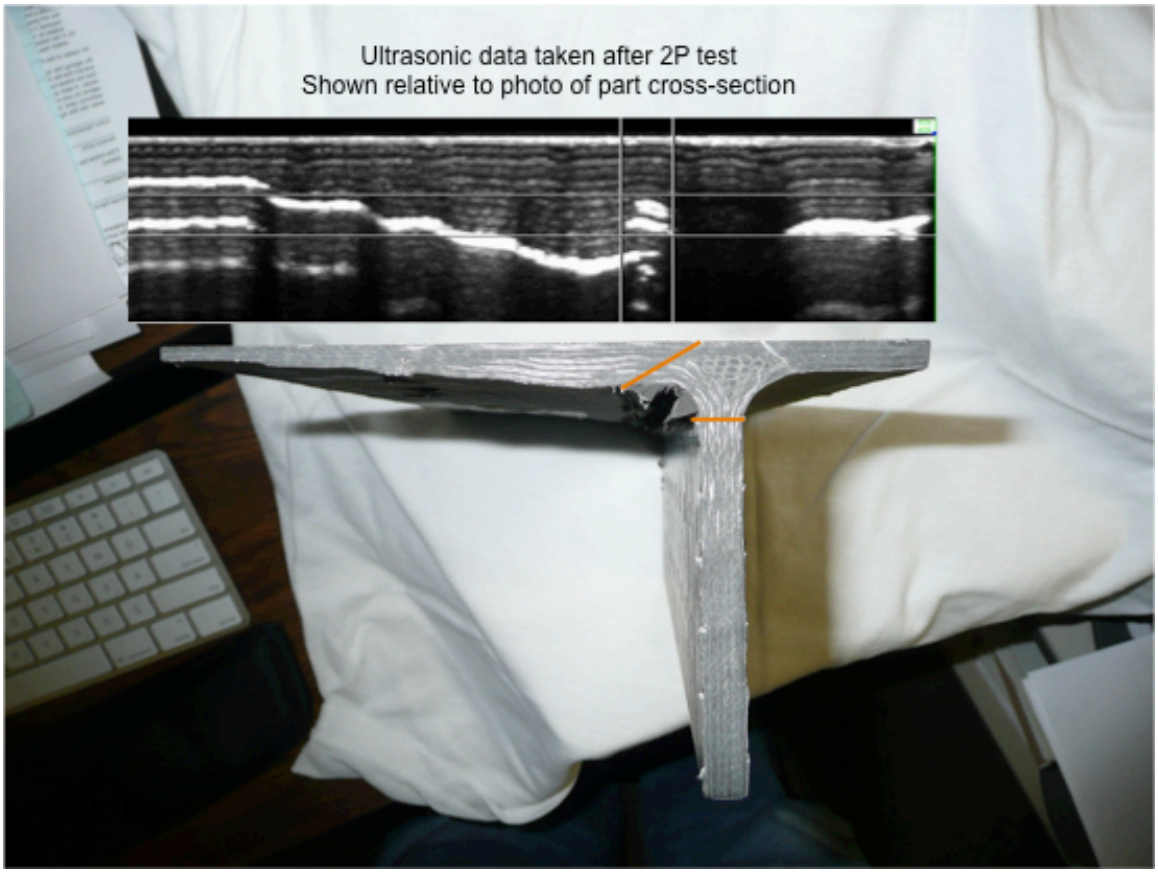

Figure 4.17. Photograph of the end of cut-out Side A, with ultrasonic B-scan data taken following the 2P test superimposed in approximate alignment.

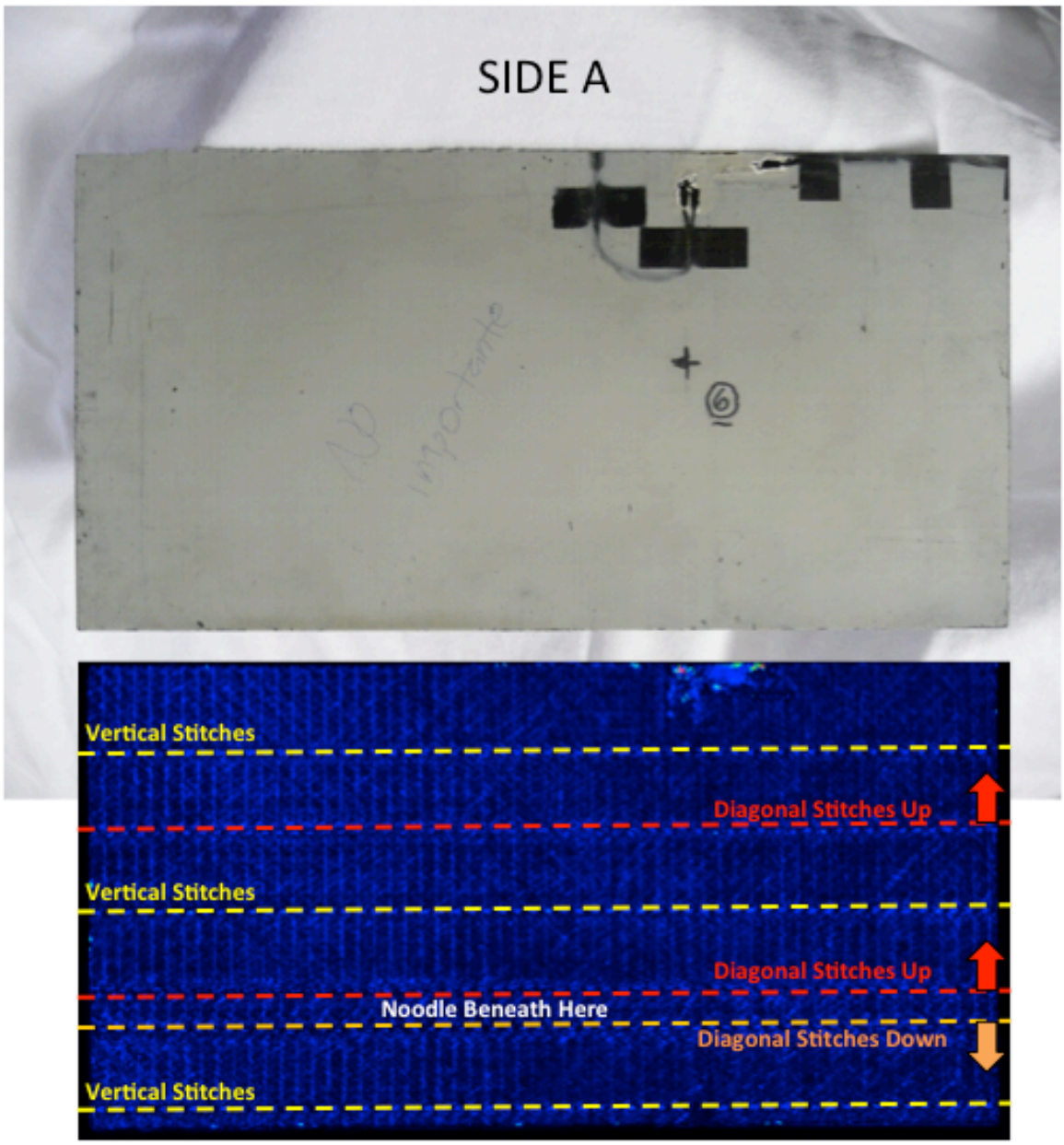

Figure 4.18. Photograph of the external surface of cutout Side A, above an ultrasonic C-scan. The C-scan was from data gated just below the surface of the part, where echoes were observed corresponding to the surface stitch material. Colored dashed lines indicate the stitch rows. Yellow lines correspond to vertically oriented stitches. Red and orange correspond to the angles stitch rows. Arrows indicate the lateral direction of the angled stitches: red in the inboard direction and orange in the outboard direction. The diagonal stitches on either side of the noodle angle away from the centerline of the end cap, as indicated in Fig. 4.17.

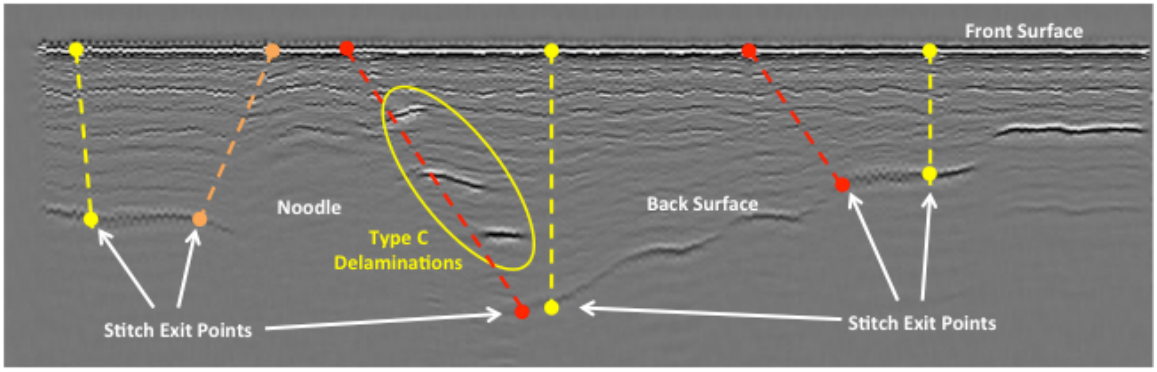

Figure 4.19. Ultrasonic B-scan through the noodle region of cut-out Side A. Using ultrasonic indications of the entry points of stitches at the top surface and bottom surface, lines are drawn to indicate approximate locations of stiches through the thickness of the specimen. Two observations of note can be made. Firstly, the Type C delaminations observed fall within the area between the red diagonal stitch and the yellow vertical stitch. Secondly, the extent of the very nearly echo-free area falls close to the diagonal stitch on either side of the noodle.

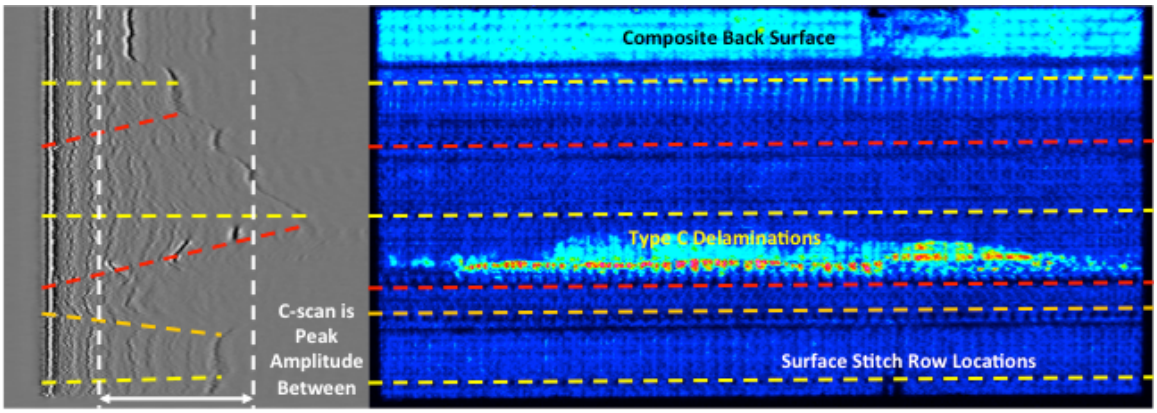

Figure 4.20. The B-scan from Fig. 4.19 rotated 90° CCW, is reproduced on the left hand side of this figure. To the right is a C-scan of the panel, made from the reflected data from the interior of the composite. The dashed colored lines, as in Fig. 4.18, represent the stitch rows at the skin surface. The indications of Type C delaminations are observed to fall within the volume of composite between the yellow vertical stitch and the red diagonal stitch line.

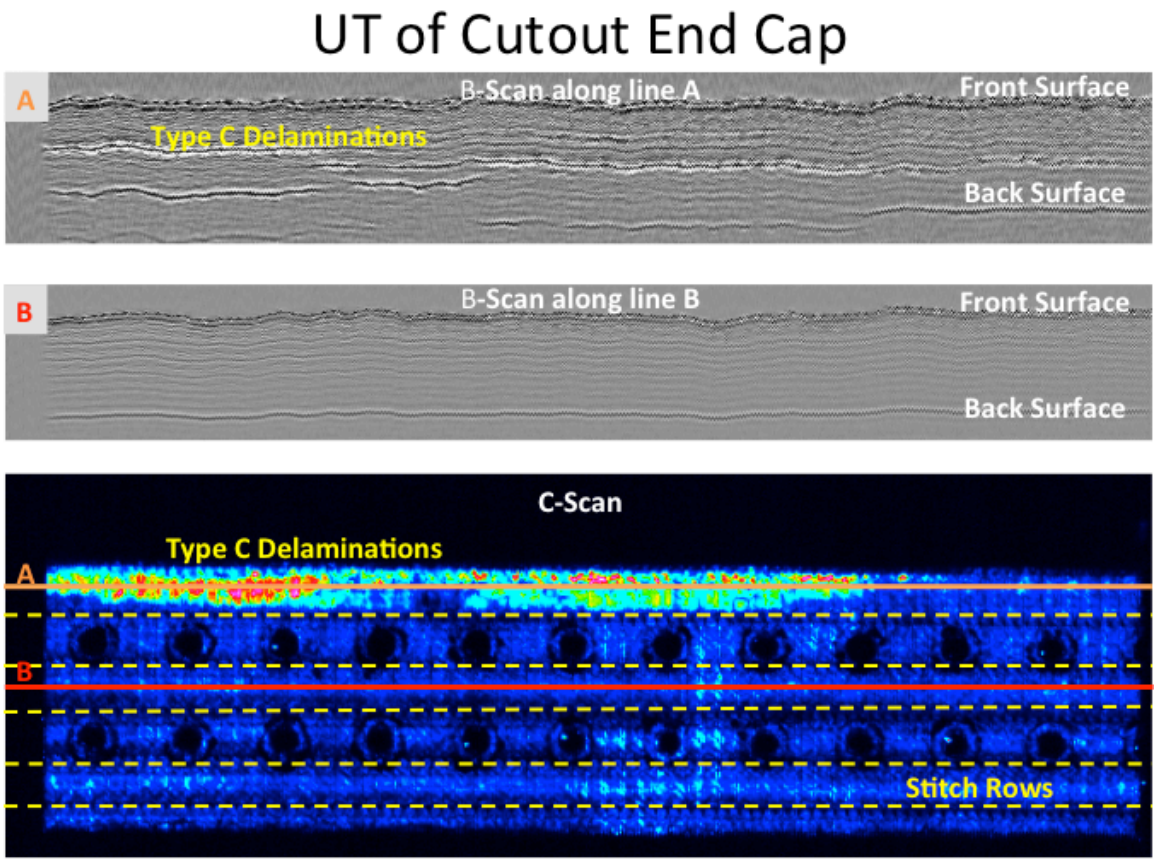

Figure 4.21. Ultrasonic scan of end cap.

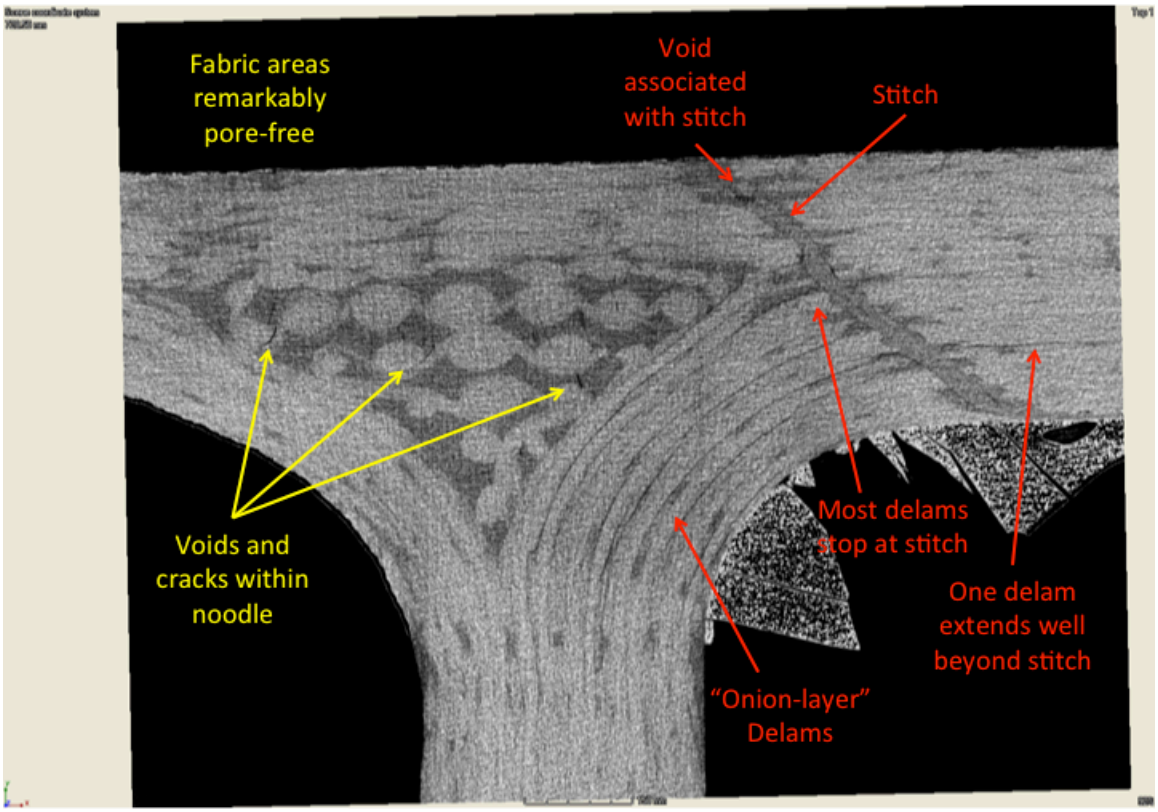

Figure 4.22. X-ray CT slice showing noodle and inner fillet region.

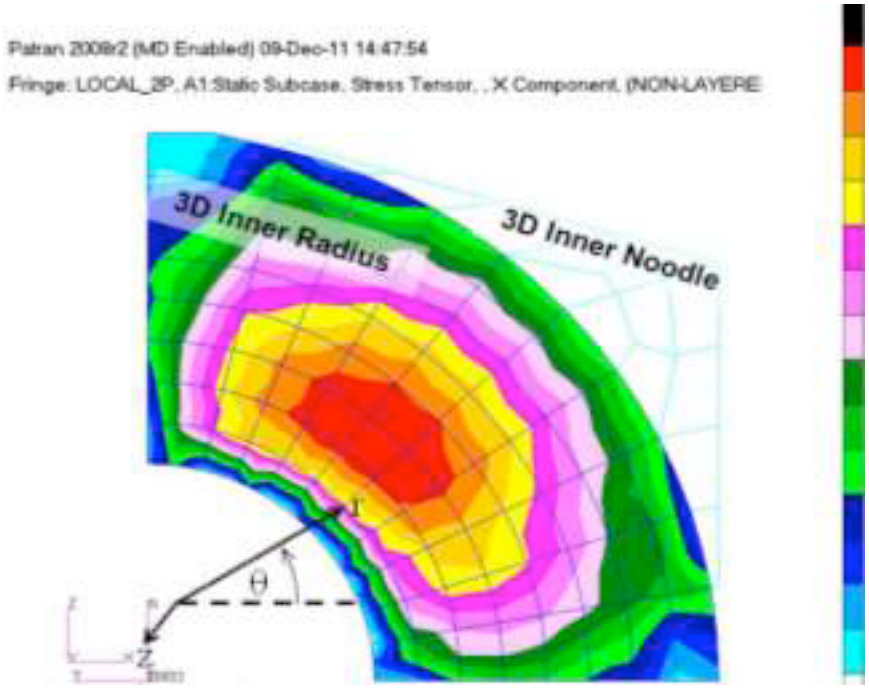

Figure 4.23. High out-out-plane stresses were predicted by analysis within inner fillet of end cap [4].

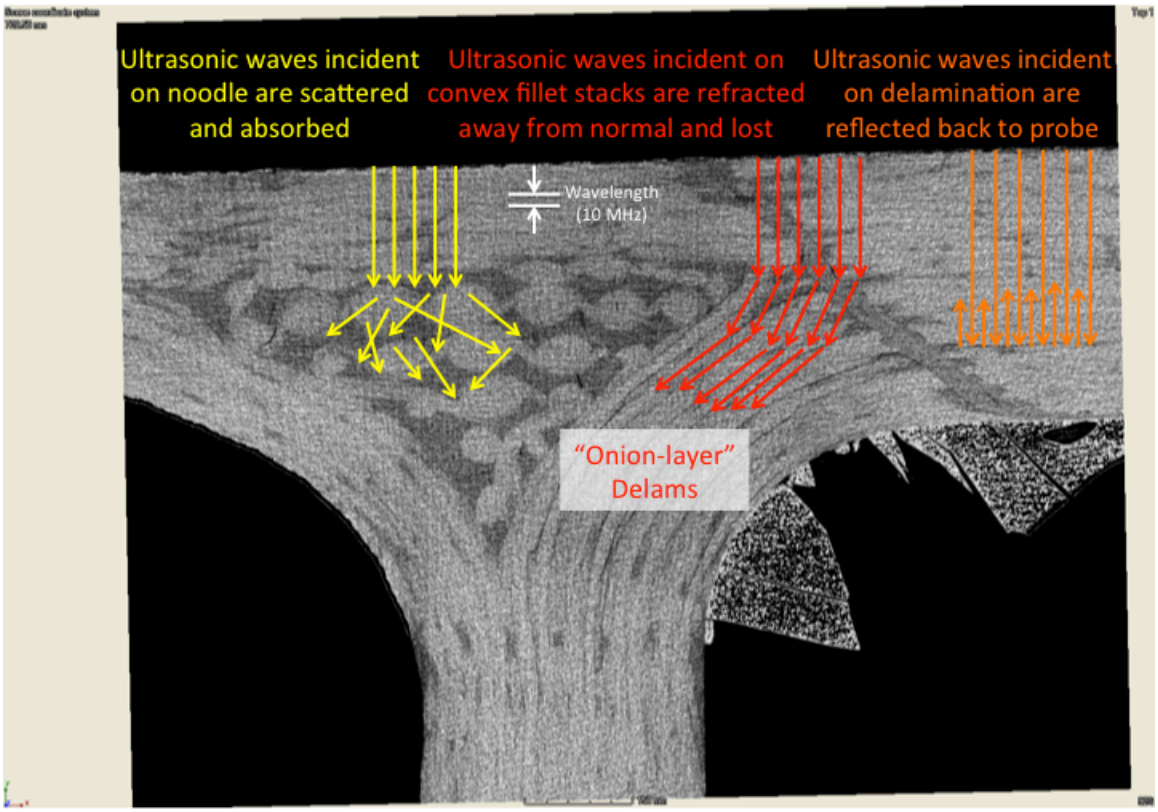

Figure 5.1. X-ray CT slice with superimposed ultrasonic ray tracings to schematically explain the interpretation of ultrasonic data.

REPORT DOCUMENTATION PAGE

Form Approved
OMB No. 0704-0188

1. REPORT DATE *(DD-MM-YYYY)*	2. REPORT TYPE	3. DATES COVERED *(From - To)*
01- 05 - 2013	Technical Memorandum	

4. TITLE AND SUBTITLE

Ultrasonic Nondestructive Evaluation of PRSEUS Pressure Cube Article in Support of Load Test to Failure

5a. CONTRACT NUMBER

5b. GRANT NUMBER

5c. PROGRAM ELEMENT NUMBER

6. AUTHOR(S)

Johnston, Patrick H.

5d. PROJECT NUMBER

5e. TASK NUMBER

5f. WORK UNIT NUMBER

699959.02.08.07.03

7. PERFORMING ORGANIZATION NAME(S) AND ADDRESS(ES)

NASA Langley Research Center
Hampton, VA 23681-2199

8. PERFORMING ORGANIZATION REPORT NUMBER

L-20216

9. SPONSORING/MONITORING AGENCY NAME(S) AND ADDRESS(ES)

National Aeronautics and Space Administration
Washington, DC 20546-0001

10. SPONSOR/MONITOR'S ACRONYM(S)

NASA

11. SPONSOR/MONITOR'S REPORT NUMBER(S)

NASA/TM-2013-217799

12. DISTRIBUTION/AVAILABILITY STATEMENT

Unclassified - Unlimited
Subject Category 24
Availability: NASA CASI (443) 757-5802

13. SUPPLEMENTARY NOTES

14. ABSTRACT

The PRSEUS Pressure Cube Test was a joint development effort between the Boeing Company and NASA Langley Research Center, sponsored in part by the Environmentally Responsible Aviation Project and Boeing internal R&D. This Technical Memorandum presents the results of ultrasonic inspections in support of the PRSEUS Pressure Cube Test, and is a companion document with the NASA test report and a report on the acoustic emission measurements made during the test.

15. SUBJECT TERMS

PRSEUS; composites; ultrasonic NDE

16. SECURITY CLASSIFICATION OF:			17. LIMITATION OF ABSTRACT	18. NUMBER OF PAGES	19a. NAME OF RESPONSIBLE PERSON
a. REPORT	b. ABSTRACT	c. THIS PAGE			STI Help Desk (email: help@sti.nasa.gov)
					19b. TELEPHONE NUMBER *(Include area code)*
U	U	U	UU	41	(443) 757-5802